iScience

Article

Early-life cognitive intervention preserves brain function in aged TgF344-AD rats with sex-specific effects

Graphical abstract

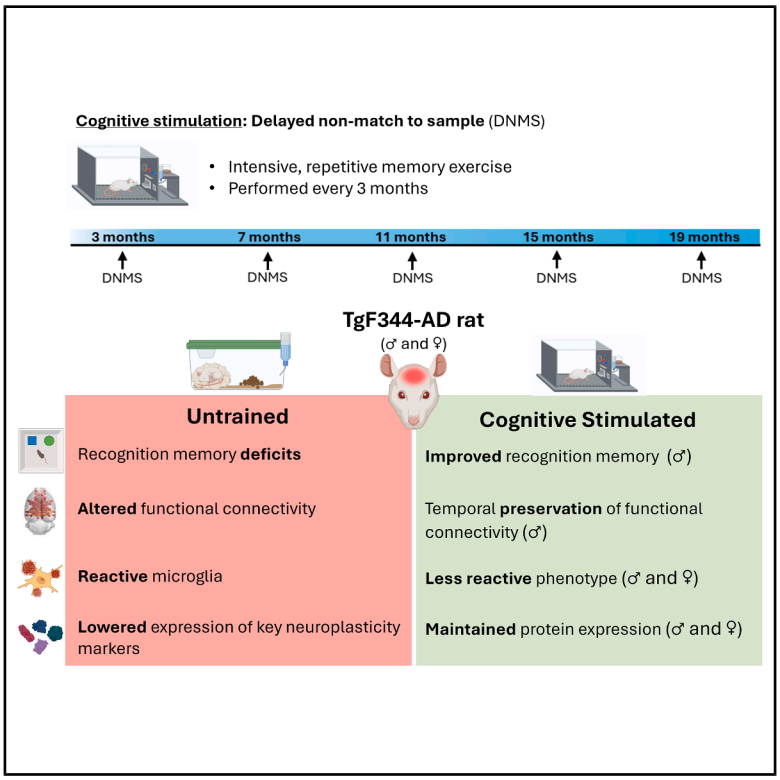

Highlights

- Early-life cognitive stimulation preserves EC and DG connectivity in TgF344-AD rats
- Cognitive training enhances memory and network resilience mainly in male transgenic rats
- Training restores synaptic plasticity markers with sex-specific molecular responses
- Cognitive stimulation transiently normalizes microglial morphology around amyloid plaques

Authors

Julia Casanova-Pagola, Federico Varriano, Xavier López-Gil, ..., Laura Molina-Porcel, Cristina Malagelada, Guadalupe Soria

Correspondence

gsoria@ub.edu

In brief

Molecular neuroscience; Cellular neuroscience; Cognitive neuroscience

Casanova-Pagola et al., 2026, iScience *29*, 114381
January 16, 2026
https://doi.org/10.1016/j.isci.2025.114381

CellPress

iScience

CellPress
OPEN ACCESS

Article

Early-life cognitive intervention preserves brain function in aged TgF344-AD rats with sex-specific effects

Julia Casanova-Pagola,[1] Federico Varriano,[1] Xavier López-Gil,[2] Genís Campoy-Campos,[3] Enric Abellí-Deulofeu,[1] Clara García-González,[1] Elisa López-Bravo,[1] Raúl Tudela,[4] Emma Muñoz-Moreno,[2] Fernando Aguado,[5] Alberto Prats-Galino,[6] Laura Molina-Porcel,[7,8] Cristina Malagelada,[3,9] and Guadalupe Soria[1,10,*]

[1]Brain Connectivity and Neuroimaging Lab, Institute of Neurosciences, Faculty of Medicine and Health Sciences, University of Barcelona, Carrer de Casanova 143, 08036 Barcelona, Spain

[2]IDIBAPS, Magnetic Resonance Imaging Core Facility, Carrer del Rosselló 149-153, 08036 Barcelona, Spain

[3]Biomedicine Department, Institute of Neurosciences, Faculty of Medicine and Health Sciences, University of Barcelona, Carrer de Casanova 143, 08036 Barcelona, Spain

[4]CIBER de Bioingeniería, Biomateriales y Nanomedicina, Instituto de Salud Carlos III, Avenida Monforte de Lemos 3-5, 28029 Madrid, Spain

[5]Department of Cell Biology, Physiology and Immunology, Biology Faculty, University of Barcelona, Carrer Diagonal 643, 08028 Barcelona, Spain

[6]Laboratory of Surgical Neuroanatomy (LSNA), Faculty of Medicine and Health Sciences, Universitat de Barcelona, Barcelona, Spain

[7]Alzheimer's Disease and Other Cognitive Disorders Unit, Neurology Service, Hospital Clínic, I Fundació de Recerca Clínic Barcelona-Institut d'Investigacions Biomèdiques August Pi i Sunyer (FRCB-IDIBAPS) and University of Barcelona, Carrer del Rosselló 149-153, 08036 Barcelona, Spain

[8]Neurological Tissue Bank, Biobanc-Hospital Clínic-FRCB-IDIBAPS, Carrer del Rosselló 149-153, 08036 Barcelona, Spain

[9]Centro de Investigación Biomédica en Red sobre Enfermedades Neurodegenerativas (CIBERNED), Instituto de Salud Carlos III, Avenida Monforte de Lemos 3-5, 28029 Madrid, Spain

[10]Lead contact

*Correspondence: gsoria@ub.edu

https://doi.org/10.1016/j.isci.2025.114381

SUMMARY

Alzheimer's disease is characterized by progressive cognitive decline, and its effects are mitigated by cognitive reserve. We investigated whether long-term cognitive stimulation, initiated before amyloid deposition, preserves brain function in male and female TgF344-AD rats. Transgenic and wild-type (WT) rats underwent cognitive training or remained untrained. Resting-state fMRI assessed functional connectivity, the novel object recognition test evaluated memory, and molecular analyses examined synaptic plasticity, inhibitory signaling, and microglial reactivity. At baseline, females showed greater task engagement and higher synaptic protein levels (PSD95, TrkB, and VGLUT) than males. Cognitive training improved connectivity and memory in males, with limited benefits in females. At 19 months, trained transgenic rats maintained entorhinal-hippocampal connectivity resembling WT rats, with males showing sustained plasticity markers and reduced parvalbumin-positive interneurons. Trained 11-month-old rats showed enhanced microglial recruitment to plaques and a less reactive phenotype. Overall, early and sustained cognitive stimulation enhances brain resilience, with sex-specific mechanisms shaping outcomes.

INTRODUCTION

Alzheimer's disease (AD) is a neurodegenerative disorder and the main cause of dementia worldwide. It is characterized by a progressive and irreversible decline in cognitive function and impaired hippocampus-dependent learning and memory. Currently, over 50 million people suffer from dementia globally, and its prevalence is predicted to triple by 2050.[1] In the absence of effective therapies, early detection, advances in diagnosis, and the application of treatments that can delay symptomatic presentation are urgently needed.

Substantial evidence shows that socio-behavioral proxies such as years of education, activities of daily living, physical exercise, and environmental enrichment are associated with less cognitive decline, cognitive flexibility, and a reduced risk of dementia in AD, possibly by increasing the threshold at which deterioration manifests clinically.[2–4] These engaging activities contribute to brain health and cognitive reserve (CR), which is the ability to maintain well-preserved cognitive function despite the presence of brain deterioration, promoting resilience to pathology.[4] The concept of CR postulates that enriching experiences are functionally protective against damage, as the brain

actively copes with or compensates for pathology by either using pre-existing cognitive processing or utilizing compensatory mechanisms.[5,6] This protective effect can arise from interacting factors such as increased neuronal plasticity, more efficient synaptic connections, and modulation of neuroinflammatory processes, all culminating in enhanced CR and the capacity to cope with pathology and preserve neuronal function.[6,7] Importantly, evidence from human cohorts indicates sex-specific patterns of cognitive resilience, with women often demonstrating better episodic memory and functional outcomes despite a greater burden of AD pathology, particularly in the earlier stages of the disease.[8–10] Therefore, it is crucial to investigate the mechanisms that increase CR, as this is a promising therapeutic approach for delaying dementia onset, especially from a sex perspective. Indeed, delaying the onset of dementia by 1 year is estimated to reduce age-dependent dementia by more than 10%.[11]

Given the late onset of symptomatology and the difficulty identifying subjects in the early stages of the disease, research using transgenic animal models of AD provides a useful tool to improve our understanding of the mechanisms and identify potential new targets to treat AD. The highly translational TgF344-AD (TG) rat model of AD recapitulates the main hallmarks of AD pathology in an age-dependent manner, as observed in patients. Specifically, TG rats develop progressive cerebral amyloid beta (Aβ) accumulation preceding tauopathy, gliosis, neuronal death, and cognitive impairment.[12]

Although the original characterization by Cohen et al., in 2013, did not detect sex differences across core measures of pathology and cognition, subsequent studies have consistently reported sex-dependent trajectories in TgF344-AD rats. Female TG rats often outperform males in hippocampal- and spatial memory-based tasks such as the active place avoidance task and the Morris water maze, particularly at early to mid-stages of disease (9–11 months), suggesting a transient cognitive resilience despite comparable or even greater Aβ burden.[13–15] At the same time, females display increased anxiety-like behaviors and reduced motivational states relative to males.[15–17] These findings may appear to diverge from clinical observations, where AD is more prevalent and often more severe in women.[18] Conflicting patterns in the literature may, in part, reflect demographic and biological differences: women's longer life expectancy contributes to higher lifetime dementia risk, whereas the impact of sex-related differences in incidence remains unclear.[19] Together, these findings underscore sex as a critical biological variable shaping AD trajectory and resilience.

Previously, we used noninvasive magnetic resonance imaging (MRI) techniques to characterize changes in functional and structural global brain connectivity in the TgF344-AD rat model.[20,21] Aging significantly affected structural network metrics in TG rats, whereas wild-type (WT) rats were stable over time. In contrast, whole-brain network metrics describing integration and segregation of the functional connectomes were unaffected.[21] In-depth characterization of resting-state networks in the same cohort revealed significant alterations in the somatosensory and default mode networks of TG rats only at early and late stages (5 and 18 months, respectively), while in mid-life stages (8, 11, and 15 months), the networks remained stable.[22] Because all animals in that study were trained on the delayed non-match-to-sample (DNMS) task, we hypothesized that repeated task engagement promoted cognitive resilience, transiently stabilizing functional networks during this period. This hypothesis directly motivated the current study.

Working memory is a key function underlying higher order domains, shown to correlate significantly with IQ in humans, and it relies on the hippocampus as well as the prefrontal and entorhinal cortices.[23,24] The DNMS task, a demanding and repetitive operant paradigm, is widely used to assess working memory because it requires sustained behavioral flexibility over time.[23,25] Based on our previous observations and the intrinsic difficulty of the task, we implemented DNMS as a form of cognitive stimulation in this study. This approach parallels other hippocampal-dependent paradigms, such as the Morris water maze, which have been employed as cognitive training interventions in AD rodent models.[26,27] While prior work has associated CR primarily with hippocampal connectivity,[28] whether the preservation of entorhinal cortex (EC) and dentate gyrus (DG) networks reflects underlying molecular and microglial adaptations remains unexplored. Our use of DNMS allowed us to address this gap by extending analyses beyond network-level metrics and integrating connectivity with molecular readouts of synaptic integrity and neuroinflammation, thereby linking brain network resilience with cellular and glial mechanisms.

According to recent guidelines, CR studies should include (1) an assessment of brain changes due to aging or disease, (2) measures of cognitive function, and (3) an identified proxy or mechanism that moderates the impact of brain pathology on cognition.[6] Taking these principles into account, we investigated whether intensive training and repetitive testing of DNMS throughout life increases CR (Figure 1). We assessed brain connectivity using MRI-based metrics and memory performance through the novel object recognition (NOR) test, allowing us to establish a link between brain function and cognitive outcomes. At the cellular level, we investigated parvalbumin (PV) expression in hippocampal interneurons and quantified synaptic proteins in the cortex as molecular readouts of synaptic integrity, a key determinant of cognitive resilience. Furthermore, we characterized microglial profiles by measuring both their morphology and their density around Aβ plaques, since these neuroinflammatory events could mediate CR in neurodegenerative conditions. To our knowledge, this is the first study to directly connect the preservation of EC and DG connectivity with molecular and microglial correlates of CR, while also addressing sex-dependent differences in these mechanisms.

RESULTS

Repetitive DNMS task performance in male and female TgF344-AD rats

To induce long-term cognitive stimulation, rats in the trained groups underwent repeated performance of the DNMS task in operant chambers. At 3 months of age, animals underwent a habituation period and six training phases with increasing levels of difficulty before the start of the DNMS task itself. The DNMS task was initiated when acquisition criteria were satisfied: 2 consecutive days with a score of a minimum of 80% correct

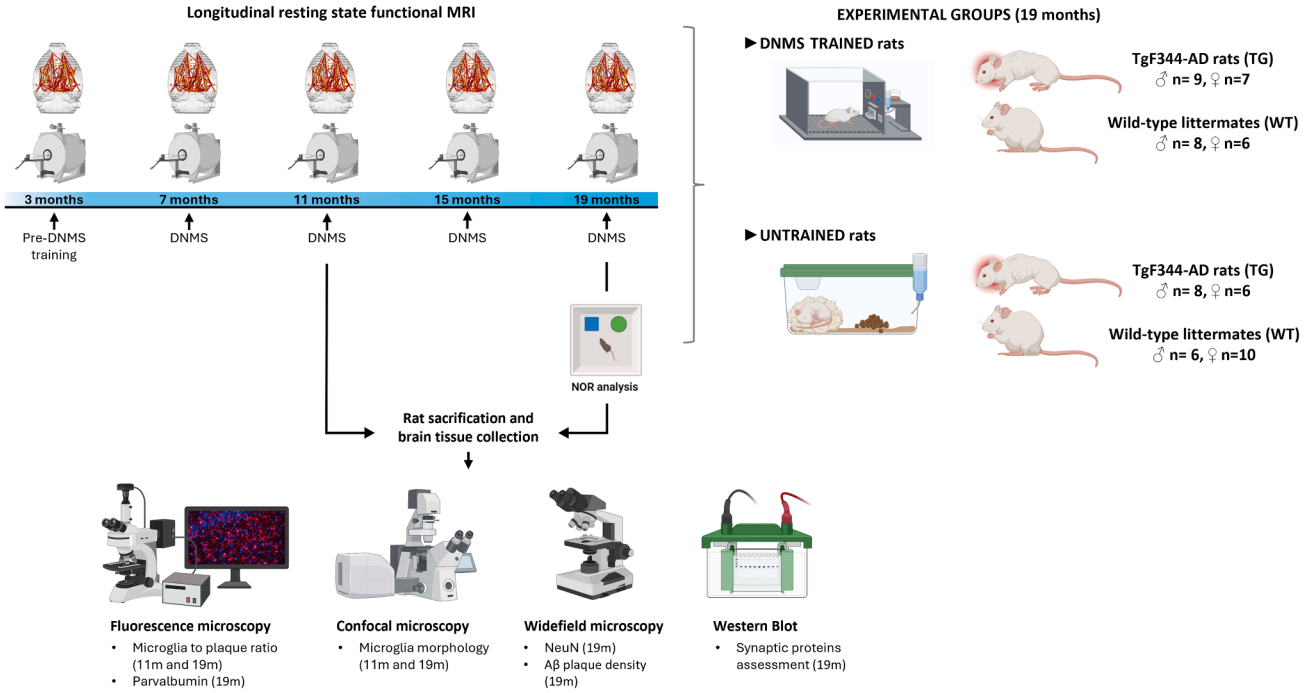

Figure 1. Schematic representation of the experimental timeline

All animals underwent an initial MRI scan at 3 months of age. They were then divided into four experimental groups: WT and TG, with or without training and periodic execution of the DNMS task. Follow-up scans were performed in all groups at 7, 11, 15, and 19 months. The NOR test was conducted at 19 months to evaluate recognition memory. A reduced subset of animals was sacrificed at 11 months (n = 4–5 rats per experimental group), while the remaining animals were sacrificed at 19 months. In both cases, brains were extracted for histological and biochemical analyses. Figure created with BioRender.

responses in the 5th and 6th training phases, where the procedure is identical to DNMS but with no delay or a delay between 1 and 5 s, respectively. All animals achieved the criteria and reached the DNMS phase, which was then performed at 7, 11, 15, and 19 months of age. A full description of the habituation, training phases, and performance criteria is provided in the STAR Methods section.

Thus, we examined the repetitive performance (7, 11, 15, and 19 months of age) of the DNMS task in male and female TG rats and their WT littermates (trained groups) by means of the number of trials performed during the task and the ratio of correct responses (Figure S1). This allowed us to monitor both motivation (trials completed) and task execution (accuracy) longitudinally. Three-way ANOVAs revealed significant interactions between sex and genotype ($p < 0.05$), sex and age ($p < 0.001$), and age and genotype ($p < 0.05$), as well as main effects of age ($p < 0.05$) and genotype ($p < 0.01$). In males, post hoc analyses indicated that TG rats performed significantly fewer trials than WT counterparts at 7 months, replicating previous findings in studies limited to males.[20,22] With aging, male WT rats showed a gradual decline in the number of trials, consistent with reduced motivation over time. By contrast, female rats displayed a different temporal pattern than males. TG females showed an inverted U-shaped curve, with trial numbers peaking at 15 months before declining again, while WT females remained stable across ages. This indicates that female rats engaged differently with the task compared to males, with TG females showing a transient increase in performance before decline.

Importantly, despite differences in the number of trials, no significant genotype effects were found in task accuracy (ratio of correct responses; Figure S1). Thus, all groups could perform the DNMS task adequately. This supports the validity of using repetitive DNMS as a paradigm for sustained cognitive stimulation.

Cognitive stimulation enhances whole-brain functional connectomics in male TgF344-AD and WT rats

To determine whether long-term cognitive stimulation, through training and repetitive DNMS performance, influenced whole-brain connectivity and organization, both untrained and trained TG and WT rats underwent a longitudinal MRI study, with a basal acquisition at 3 months of age and at later time points (7, 11, 15, and 19 months of age) after DNMS task performance (Figure 1).

Since integration and segregation are two fundamental principles of brain organization, we computed the global efficiency and clustering of the resting state (rs)-fMRI connectome (Figure 2). A three-way ANOVA revealed a significant interaction between age and treatment ($p < 0.05$) and a significant main effect of age ($p < 0.01$; $p < 0.001$) and treatment ($p < 0.001$) on the global efficiency and clustering in male rats, respectively (Figures 2A and 2C). Although no significant differences were observed between genotypes, this analysis revealed different temporal patterns of integration and segregation aspects of functional connectivity among the treatment groups in both WT and TG rats. Notably, post hoc analyses showed that at both 7 and 11 months of age, male trained rats had significantly higher global efficiency compared to their untrained littermates

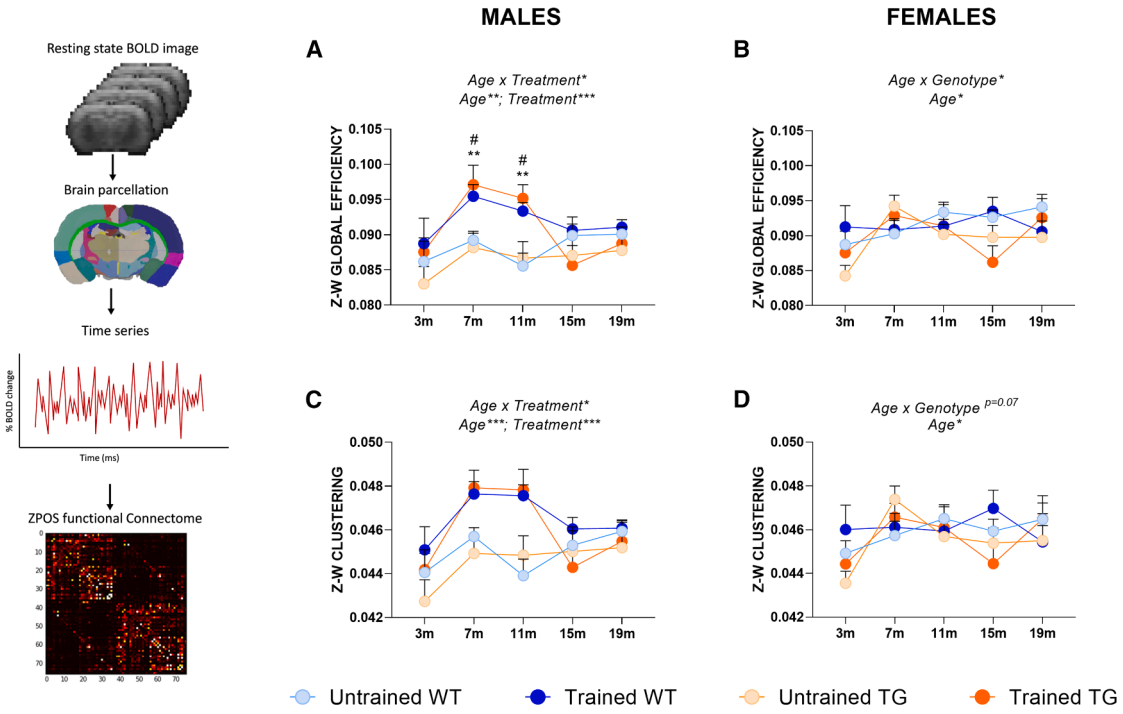

Figure 2. Whole-brain functional connectomics are preserved in cognitively stimulated male TG rats

Data show global efficiency (A and B) and clustering (C and D). The effects of genotype, treatment, and age, as well as the interactions between these factors, were assessed using mixed-effect analyses and Tukey's multiple comparisons test. N = 5–6 rats per experimental group. Data are expressed as the average metric value ±SEM *$p < 0.05$; **$p < 0.01$; ***$p < 0.001$, and #$p < 0.05$. Significant differences between treatment groups within each time point are denoted with "#" for WT rats and "*" for TG rats. Full statistical details are available in Table S2.

(WT, $p < 0.05$; TG, $p < 0.01$, at both time points) (Figure 2A). In female rats, a three-way ANOVA revealed a significant interaction between age and genotype ($p < 0.05$) in global efficiency and a significant effect of age ($p < 0.05$) in both global efficiency and clustering (Figures 2B and 2D, respectively). Thus, no effect of cognitive stimulation was observed in females, either globally or at any time point. Full statistical details are available in Table S2.

Cognitive stimulation restored the functional connectivity of EC and DG in TgF344-AD rats

As whole-brain connectomics evidenced increased metrics in the trained groups (WT and TG) without genotype effects in the untrained groups, we next performed seed-based analyses to study the connectivity of critical regions in AD pathology: the DG of the hippocampus and the EC.

Seed-based analyses allow the study of correlations between the activity of the region of interest (seed) and the rest of the brain and require a large sample size, limiting us to combining males and females for the analysis. EC seed-based analyses revealed genotype-specific differences in the functional connectivity maps of untrained rats, as shown in the average connectivity maps of WT and TG animals (Figure 3A). The statistical maps showed brain regions where functional connectivity was significantly lower in TG rats compared to WT littermates, which included the visual, somatosensory, motor, cingulate, and retrosplenial cortices (WT > TG; $p < 0.05$, FWE-corrected) (Figure 3A). These baseline connectivity dysfunctions were corrected in the trained group, as the averaged connectivity maps showed very similar patterns between genotypes. In fact, no significant differences were observed in the statistical map, suggesting that cognitive stimulation prevents this network deterioration (Figure 3B).

Similar results were obtained when the seed was located in the DG of the hippocampus (Figures 3C and 3D). In untrained TG animals, we found hypoconnectivity of the DG with the rest of the brain compared to their WT counterparts, especially with areas such as the contralateral somatosensory and visual cortices and the contralateral hippocampus, as revealed by the statistical maps (Figure 3C). Once again, trained WT and TG rats showed similar connectivity of the DG, as evidenced by the lack of significant voxels in the statistical map (Figure 3D).

Hence, these findings underscore the potential of cognitive stimulation as a preventive strategy against network deterioration in AD, highlighting its ability to normalize functional connectivity patterns in TG rats to levels comparable with those of their WT littermates.

Cognitive stimulation prevents recognition memory deficits in 19-month-old male TgF344-AD rats

Next, we assessed whether the observed protective effect of the training paradigm extended to cognitive performance. For this purpose, we evaluated recognition memory using the NOR test. This task measures hippocampal-dependent

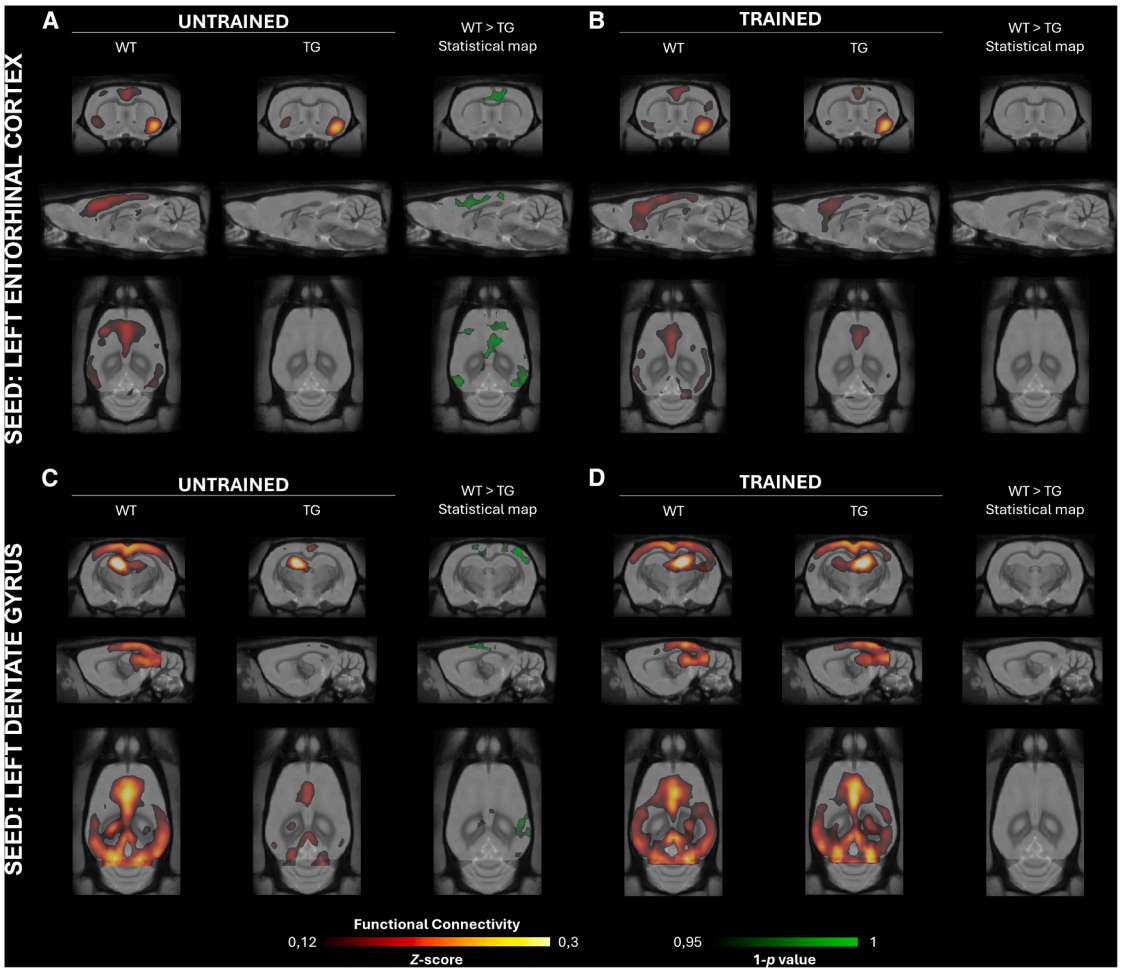

Figure 3. Seed-based analyses of the EC and DG reveal restored functional connectivity in trained TG rats

Seed-based connectivity analyses were performed on the left EC and left DG. Average functional connectivity maps per genotype (left and center) and statistical maps indicating significant family-wise error-corrected differences (right) are shown for untrained (A and C) and trained (B and D) rats (WT > TG; $p < 0.05$, FWE-corrected). N = 10–12 rats per experimental group. The image's left is the animal's right.

recognition memory, which is particularly vulnerable to deterioration in dementias such as AD.[29] The NOR paradigm is based on rodents' innate tendency to explore novel objects more than familiar ones, indicating retention of a memory trace for the familiar stimulus. Thus, at 19 months of age, including both sexes, a two-way ANOVA revealed a significant effect of treatment ($p < 0.05$), with trained rats showing a higher recognition index (RI), and a near-significant effect of genotype ($p = 0.0536$), with TG rats performing worse (Figure 4A). When including the effect of sex in the analysis, a three-way ANOVA revealed a significant effect of treatment ($p < 0.05$) on RI, a near-significant effect of genotype ($p = 0.0526$), and no effect of sex. As shown in Figure 4B, training particularly improved the RI of male rats, with TG males showing a significant increase compared to their untrained counterparts ($p < 0.05$). In contrast, TG females did not benefit from repeated DNMS task performance, showing no observable improvement in recognition memory. Of note, a significant effect of training ($p < 0.05$) was also observed in the total exploration time during the NOR test, with all trained groups except female TG rats exploring more than their untrained counterparts (Figure S2).

In addition, using a one-sample t test, we compared the RI of each group against chance level (50%) to determine whether animals performed above chance (indicating true recognition of novelty) or below (suggesting a preference for the familiar object). This analysis confirmed that WT-trained rats performed significantly above chance ($p < 0.05$), whereas TG untrained animals scored below chance ($p < 0.05$). When sexes were analyzed separately, only female trained WT animals performed significantly above chance ($p < 0.001$), indicating true recognition memory at 19 months. Importantly, TG-trained males did not differ from chance ($p = 0.14$), while their untrained counterparts scored nearly below chance ($p = 0.078$), suggesting a preference for the familiar object. At 19 months of age, rats show limited exploration (Figure S2), which can make the NOR task difficult to interpret. In this context, performance at chance is itself informative, as it indicates that animals explore both objects equally and is therefore preferable to being below chance.

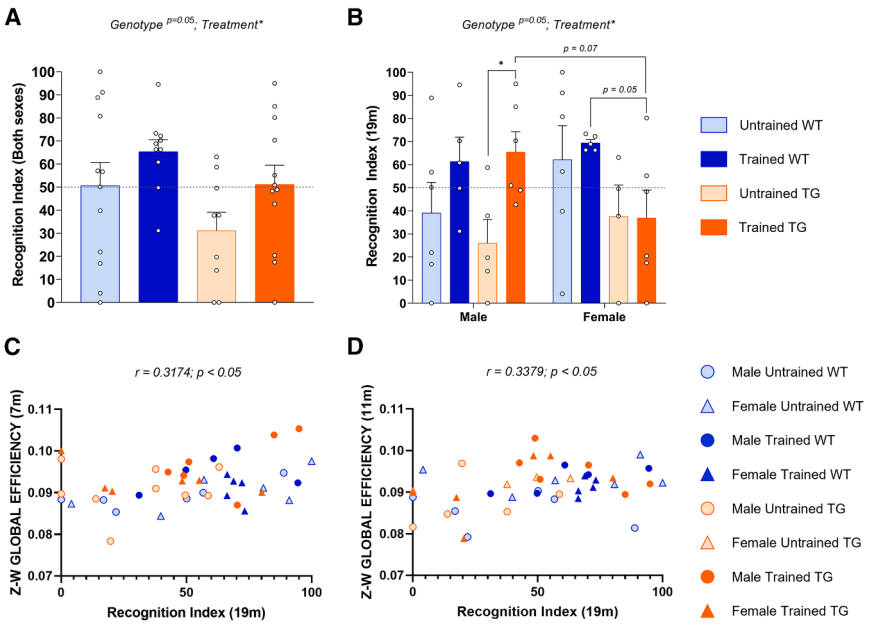

Figure 4. Recognition memory is preserved in aged male TG rats as a consequence of cognitive stimulation and is correlated with functional connectivity measures

(A) Recognition memory was assessed in 19-month-old rats using the RI, the time spent in the novel object relative to total object exploration. An RI greater than 50% indicates a novelty preference. The effects of genotype and treatment and the interactions between these factors were assessed by a two-way ANOVA with Tukey's post hoc tests; N = 9–12 rats per group when sexes were combined.

(B) RI was also analyzed separately by sex, where the effect of genotype, treatment, and sex, and the interactions between these factors, were assessed by a three-way ANOVA followed by Fisher's LSD test. N = 4–6 rats per experimental group. Data are presented as mean ± SEM; *p < 0.05. The dashed line at 50% represents chance level.

(C and D) Pearson's correlations between the global connectivity at 7 (C) and 11 (D) months of age and RI at 19 months. Significant positive correlations were observed at both time points (C: r = 0.3174; p = 0.0381; D: r = 0.3379; p = 0.0267). See also Figure S2 and Table S3 for the full statistical details.

Accordingly, these results support that long-term training mitigated recognition memory decline in TG rats, particularly in males.

To further explore the relationship between early-life network changes and long-term cognitive performance, we performed a correlation analysis between RI at 19 months and functional connectivity metrics derived from rs-fMRIs at 7 and 11 months. As previously described, at these two specific time points, TG males subjected to cognitive stimulation exhibited significantly higher values of global efficiency compared to untrained TG males. Notably, higher connectomic metrics significantly correlated with recognition memory performance at 19 months (r = 0.3174; p < 0.05 and r = 0.3379; p < 0.05, respectively; Figures 4C and 4D). These findings suggest that cognitive stimulation may induce lasting functional reorganization of brain networks with an impact on recognition memory, supporting the relevance of network-level biomarkers as early indicators of resilience to cognitive decline in transgenic models of AD.

Cognitive stimulation significantly decreased the expression of PV in DG interneurons

Given the observed differences in recognition memory performance, particularly the selective improvement in TG males following cognitive stimulation, we investigated whether these effects were associated with protective effects on neurodegeneration in the hippocampus and the EC. Neuronal density analyses revealed a limited effect of genotype in the DG (Figure S3).

Since PV-positive (PV^+) interneurons have a crucial role in memory encoding and regulation of network oscillations and plasticity,[30] we next explored the impact of long-term cognitive stimulation on hippocampal inhibitory circuitry by quantifying PV expression in interneurons of the CA1, CA3, and DG regions (Figure 5A). Three-way ANOVAs revealed a significant effect of genotype in the CA3 (p < 0.05), with reduced PV expression in TG rats compared to WT (Figure 5C). Moreover, a significant effect of treatment was observed in the DG (p < 0.01), where trained rats (both WT and TG) showed significantly less PV expression (Figure 5D). Subsequent post hoc analyses revealed a significant decrease in PV expression in DG interneurons of male trained WT rats (p < 0.05) compared to their untrained littermates. These findings demonstrate that genotype and cognitive stimulation independently alter hippocampal inhibition, suggesting a potential mechanism of experience-dependent inhibitory plasticity in the hippocampus, which may contribute to the observed differences in recognition memory performance.

Cognitive stimulation restored the expression of neuroplasticity proteins in male TgF344-AD rats

To investigate whether cognitive stimulation contributed to the preservation of neuronal plasticity, the levels of synaptic proteins (PSD95, TrkB, and VGLUT) and neuroplasticity-related proteins (p-RPS6 and RPS6) were assessed in the cortex of 19-month-old rats (Figures 6 and S4). The lysates included the motor, somatosensory, auditory, insular, and entorhinal cortices; these regions showed altered connectivity in the seed-based analyses of both the EC and DG in the untrained TG rats. Corresponding membrane immunoblots used for densitometries can be found in Figure S5.

Three-way ANOVAs revealed a near-significant sex × genotype × treatment interaction in the relative expression of PSD95 and TrkB (p = 0.0551 and 0.0592, respectively) (Figures 6A and 6B) and a significant triple interaction in the relative expression of VGLUT (p < 0.05) (Figure 6C). In addition, a significant genotype × treatment interaction was revealed in the

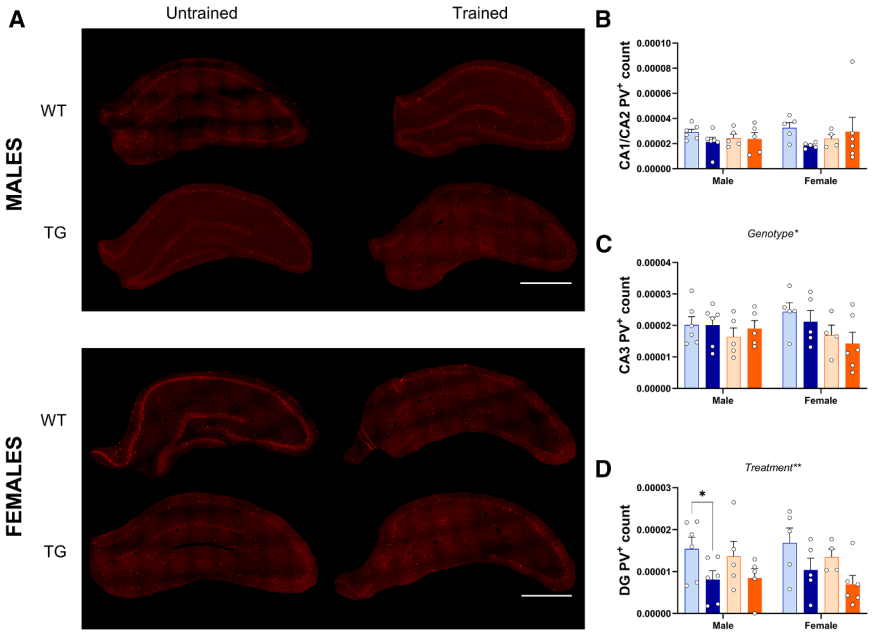

Figure 5. Relative PV expression in 19-month-old rats

(A) Representative immunofluorescence image of PV^+ interneurons in the DG (red).

(B–D) For each experimental group, PV^+ interneuron numbers in the B) CA1/CA2, C) CA3, and D) DG were obtained and normalized to the area of each region. The effects of sex, genotype, and treatment were assessed by a three-way ANOVA followed by Fisher's LSD test. The scale bar represents 1 mm. N = 4–6 rats per experimental group. Data are presented as mean ± SEM; $^*p < 0.05$; $^{**}p < 0.01$.

Full statistical details are available in Table S4.

relative expression of VGLUT ($p < 0.05$) and p-RPS6 ($p < 0.01$) (Figure 6C and 6D). Moreover, a significant effect of sex was found in PSD95, TrkB, and VGLUT ($p < 0.05$, $p < 0.01$, and $p < 0.01$, respectively) (Figures 6A–6C), and a significant effect of genotype was observed in TrkB ($p < 0.001$) (Figure 6B). Post hoc analyses revealed basal sex-dependent differences in untrained TG rats, where female rats had significantly higher expression of PSD95, TrkB, and VGLUT compared to males ($p < 0.001$, $p < 0.01$, and $p < 0.001$, respectively) (Figures 6A–6C). Overall, male untrained TG rats had lower expression of key neuroplasticity markers, including PSD95, TrkB, and p-RPS6, compared to male untrained WT rats ($p < 0.01$, $p < 0.01$, and $p < 0.05$, respectively) (Figures 6A–6D). Cognitive training restored the protein expression of PSD95 and p-RPS6 in TG males to WT-like levels. Female untrained TG rats had lower expression of p-RPS6 compared to untrained WT littermates ($p < 0.01$). In line with this, trained TG females had significantly higher expression of p-RPS6 compared with their untrained littermates ($p < 0.01$) (Figure 6D), showing that training restored p-RPS6 expression to WT-like levels. Additionally, the expression of these proteins was evaluated in hippocampal lysates of the same subjects (Figure S6), where a similar trend toward increased expression of p-RPS6 in trained animals was observed (Figure S6D).

In summary, untrained rats displayed sex-dependent differences in both their protein profiles and responses to cognitive stimulation. Female untrained TG rats had higher expression of PSD95, TrkB, and VGLUT compared to their male littermates, and cognitive stimulation normalized the expression of PSD95 in male TG rats and p-RPS6 in both sexes. These findings suggest that cognitive stimulation may help preserve neuronal plasticity in TG rats, particularly in males, by restoring the expression of key synaptic and neuroplasticity-related proteins to levels comparable with WT animals.

Cognitive stimulation increases the presence of microglia around Aβ plaques and transiently preserves a WT-like microglial morphology in 11-month-old TG rats

Microglia cells have a neuroprotective role in amyloid β-protein clearance, clustering around Aβ plaques to form barriers that prevent plaque expansion and further glial activation.[31] We first investigated whether long-term cognitive stimulation reduced Aβ burden in TG rats at 19 months of age. However, we only found a trend toward reduced Aβ burden with treatment in the DG ($p = 0.0515$) (Figures S7A–S7D).

Next, we addressed the impact of cognitive training on the density of microglial cells surrounding Aβ plaques. Data were collected at two time points (at 11 and 19 months of age). The sample size at 11 months was too small to allow for sex-specific analyses, so the data are presented with sexes combined. Two-way ANOVAs were conducted in the EC, DG, CA1, and CA3 (Figure 7). A significant interaction of treatment and age was observed in the EC ($p < 0.05$), as well as a significant effect of treatment ($p < 0.01$) (Figure 7A). A significant effect of age was observed across all studied areas ($p < 0.001$ for all) (Figures 7A–7D).

In 11-month-old rats, post hoc analyses in the EC revealed a significantly greater microglial density relative to Aβ plaques in trained TG rats compared to untrained rats ($p < 0.01$) (Figure 7A), with a similar trend observed in the DG (Figure 7B). In the same line, an increase in total microglia density was observed in trained TG rats compared to trained WT rats (Figure S7E). Compared to younger rats, 19-month-old rats had a significantly lower density of microglia cells around Aβ plaques in all brain regions, irrespective of training (untrained: EC, $p < 0.001$; DG, $p < 0.01$; CA1, $p < 0.01$; CA3, $p < 0.05$; trained: EC, $p < 0.001$; DG, $p < 0.001$; CA1, $p < 0.05$; and CA3, $p < 0.05$) (Figures 7A–7D). By 19 months of age, the significant effect of cognitive training was no longer observed. Thus, cognitive stimulation enhanced the proportion of microglia surrounding plaques in an age-dependent manner, particularly in the EC, as this effect of training was not evident in older rats. Independently of treatment, by 19 months, there was a drastic decrease in microglia per Aβ plaque, suggesting that microglial function is compromised with aging.

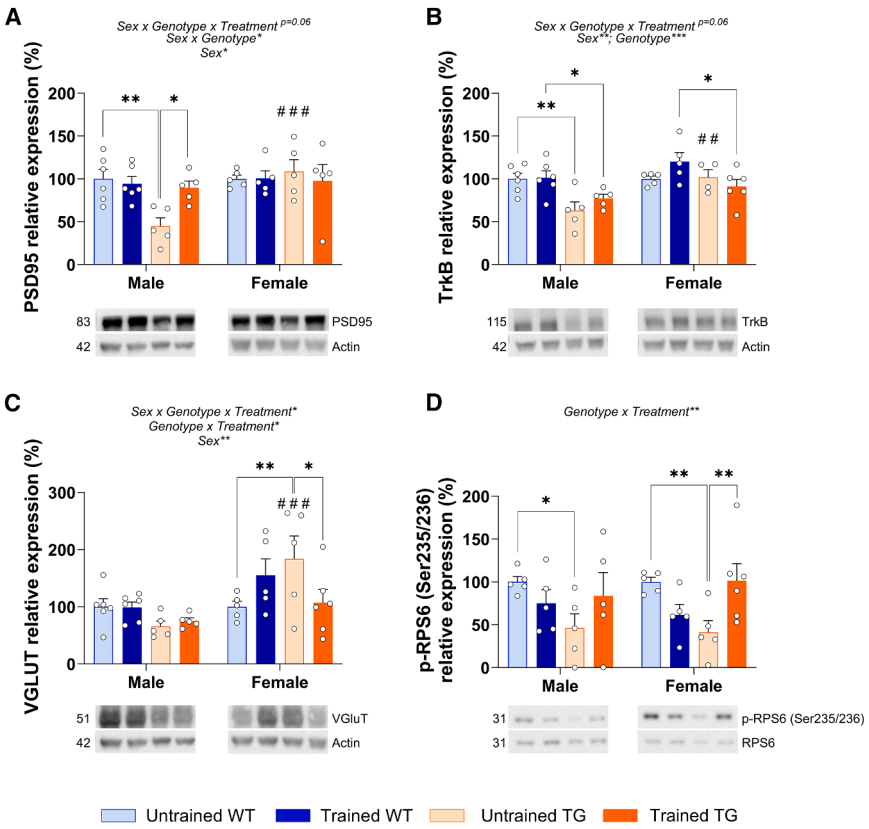

Figure 6. Cognitive stimulation prevents altered protein expression in TG rats

(A) Immunoblottings and densitometric quantifications of PSD95 normalized to actin, expressed as a percentage relative to the untrained WT conditions.

(B) Immunoblottings and densitometric quantifications of TrkB normalized to actin, expressed as a percentage relative to the untrained WT conditions.

(C) Immunoblottings and densitometric quantifications of VGLUT normalized to actin, expressed as a percentage relative to the untrained WT conditions.

(D) Immunoblottings and densitometric quantifications of p-RPS6 normalized to RPS6, expressed as a percentage relative to the untrained WT conditions. Respective molecular weight in kDa. The effects of genotype, treatment, and sex and the interactions between these factors were assessed by a three-way ANOVA followed by Fisher's LSD test. N = 5–6 rats per experimental group. Data are presented as mean ± SEM; *$p < 0.05$; **$p < 0.01$; ***$p < 0.001$ and ##$p < 0.01$; ###$p < 0.001$. Significant differences between males and females per experimental group are denoted with "#."

See also Figures S4–S6 and Table S5 for the full statistical details.

Microglia morphology serves as a crucial indicator of their functional state and reactivity, reflecting changes in activation, phagocytic capacity, and inflammatory responses.[32] Indeed, morphological analyses can reveal subtle changes in microglial function that may not be apparent through density measurements alone. Therefore, we investigated whether differences in microglia morphology (circularity and branch number) were detectable between TG and WT rats and whether cognitive stimulation impacted microglial morphology in the EC (Figure 7F). Three-way ANOVAs revealed a significant age × genotype × treatment interaction (circularity, $p < 0.01$ and branch number, $p < 0.001$), a significant interaction between age and genotype (circularity, $p < 0.05$ and branch number, $p < 0.01$), a significant interaction between genotype and treatment (branch number, $p < 0.01$), and significant main effects of age ($p < 0.001$ for both) and genotype (circularity, $p < 0.01$ and branch number, $p < 0.05$) (Figures 7G and 7H). Post hoc analyses revealed that in 11-month-old rats, microglia in untrained TG rats were more circular and less branched ($p < 0.001$ for both) (Figures 7G and 7H), suggesting a more reactive phenotype compared to untrained WT littermates. Trained TG rats had significantly less circular and more branched microglia compared to their untrained littermates ($p < 0.01$ and $p < 0.05$, respectively) (Figures 7G and 7H), resembling a WT-like phenotype. As rats aged, microglia became significantly more circular (WT untrained: $p < 0.001$ and TG untrained: $p < 0.05$) and less branched (WT untrained: $p < 0.001$; WT trained: $p < 0.05$; and TG trained: $p < 0.01$) (Figures 7G and 7H). In 19-month-old rats, the effect of long-term cognitive stimulation was lost, as no significant differences were found between treatment groups. In summary, the microglial morphology in 11-month-old trained TG rats resembles that of WT animals, being less circular and more branched. With aging, microglia became more rounded and less branched, and the effect of training dissipated. These results highlight the potential of sustained cognitive intervention to temporarily modulate microglial morphology and, potentially, their function in TG rats.

DISCUSSION

Our study uniquely examines the impact of long-term cognitive stimulation from early adulthood on both healthy and pathological aging in the TgF344-AD rat model, while also accounting for sex differences. We found clear basal differences between sexes, as females outperformed males in DNMS engagement (both WT and TG animals), and TG females displayed higher expression of key synaptic proteins (PSD95, TrkB, and VGLUT), pointing to a fundamental female advantage. Recognizing such differences is essential, as promoting healthy aging involves mitigating cognitive decline, enhancing brain function, and strengthening CR.[33] Following established research guidelines for studying CR,[6] our longitudinal study demonstrates that long-term cognitive stimulation preserves whole-brain functional connectomics and specifically EC and hippocampus connectivity, leading to improved recognition memory, particularly in male TG rats. As shown by our results, this protective effect may

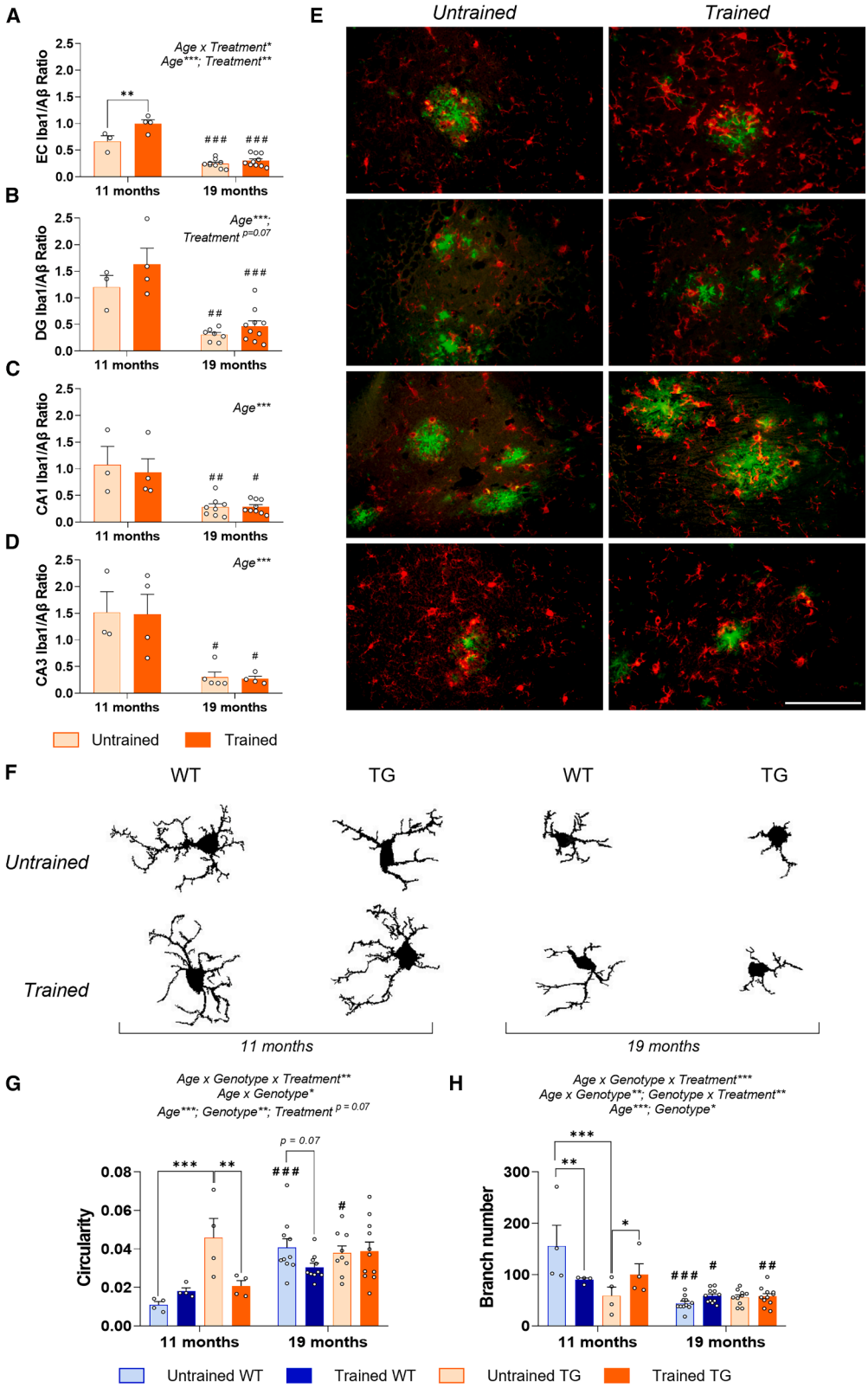

(legend on next page)

be attributed to increased expression of neuronal plasticity markers and a less reactive neuroinflammatory profile in trained rats.

Our findings highlight the relevance of network integration and segregation metrics as indicators of functional brain organization and cognitive resilience in AD and healthy aging. Increased segregation (clustering coefficient)[34] and integration (global efficiency)[35] have been associated with better cognitive outcomes and delayed decline in AD. Furthermore, greater resting-state global functional connectivity correlates with higher CR in patients with mild cognitive impairment,[36] underscoring the translational value of these metrics in early detection and intervention strategies. Importantly, our study demonstrates sex-dependent effects of early cognitive stimulation on whole-brain connectomics. In male TG animals, early stimulation enhanced network integration and segregation, particularly at 7 and 11 months of age, consistent with a protective effect on functional brain organization. A similar effect was also observed in WT males, indicating that cognitive stimulation supports functional network integrity even in the absence of pathology. By contrast, neither female TG nor WT animals exhibited sustained improvements. This aligns with clinical findings showing that women experience more pronounced dementia-related changes in functional brain connectivity[37] and structural brain damage,[19] supporting the notion of lower brain resilience in females.

These results extend prior work on functional connectivity in AD models, particularly regarding sex differences. Previous studies, including our own, reported preserved whole-brain functional connectivity in male TG rats until later disease stages, despite early changes in structural connectivity.[20,21] Within the same dataset, however, specific resting-state networks, such as the somatosensory and anterior default mode networks, showed divergent connectivity patterns in TG rats compared to WT males.[22] Other studies using dynamic rs-fMRI identified early functional disruptions in basal forebrain and default mode-like regions by 4 months of age, but these analyses were restricted to male animals.[38,39] In contrast, a separate longitudinal study of female rats reported widespread functional connectivity decline by 10 months.[40] While differences in imaging and analytic methods may partly explain variability across studies, a critical limitation remains: the lack of sex-inclusive designs. By incorporating both sexes, our work addresses this gap and offers a more comprehensive view of functional connectome dynamics in AD. Whole-brain network analyses bridge phylogenetic differences between rodent and human studies, providing a translational link between species,[41] and accounting for sex as a biological variable is essential given known differences in AD prevalence and CR mechanisms.[19]

We did not detect an overall genotype effect in whole-brain global connectomics, which may reflect compensatory mechanisms within large-scale networks. This prompted us to examine the EC, a region central to memory and especially vulnerable in AD. Seed-based analyses revealed genotype-dependent connectivity deficits in untrained TG rats, which were absent in trained animals, indicating that cognitive stimulation mitigates disease-related alterations at the circuit-specific level.

Notably, the preservation of EC and hippocampal connectivity translated into enhanced memory performance, particularly in the NOR test, which depends on cortical and hippocampal circuits. Although both the DNMS and NOR tasks assess memory, DNMS training extends its effects beyond hippocampal circuits to broader cortical areas involved in recognition memory.[26] By 19 months, WT rats typically show age-related memory decline,[42,43] while TG rats exhibit earlier and more severe impairments.[12,15,44,45] Consistent with this, untrained animals, regardless of genotype, were unable to discriminate between novel and familiar objects. However, cognitive stimulation significantly improved the recognition index (RI) in male WT and TG rats, highlighting its protective effect against memory decline in both normal and pathological aging. These results align with previous findings in AD models, where enrichment and exercise improved cognitive outcomes. Periodic cognitive enrichment enhanced memory performance in 18-month-old 3xTg-AD mice compared to nonenriched littermates,[26] and exercise protected memory function in male TgF344-AD rats and Aβ-injected Wistar rats.[46,47] Human studies similarly associate cognitive and physical activity with preserved cognition in aging and dementia.[4] Interestingly, female rats did not similarly benefit from cognitive stimulation, possibly due to a more pronounced genotype effect. Although the original characterization of the TgF344-AD rat model reported no sex differences,[12] later studies revealed that female rats in this model often outperform males in memory tasks at earlier ages, including active avoidance[13] and delayed match-to-sample tests.[16] In fact, we observed a different temporal evolution in the number of trials performed in the DNMS task from 7 to 19 months between sexes, with males showing age-related declines in motivation and TG females displaying a transient increase before decline. In the same line, a recent study evaluating the effect of aerobic exercise from 12 to 18 months of age in this rat model showed that exercise training rescued memory impairments in female transgenic rats, whereas males showed no exercise-induced improvement.[48] Altogether, this

Figure 7. Microglia-to-plaque size ratio increases in the entorhinal cortex and protects microglial morphology in 11-month-old TG rats

(A–D) Mean ratio of microglia-to-plaque size in the (A) EC, (B) DG, (C) CA1, and (D) CA3 per rat in 11- and 19-month-old TG rats (both sexes combined). The effects of treatment and age and the interactions between these factors were assessed by a two-way ANOVA with Tukey's post hoc tests. Scale bars represent 50 μm. At 11 months old, $N = 3–4$ rats, and at 19 months old, $N = 9–10$ rats per experimental group.

(E) Representative double-immunofluorescent staining of microglia ($Iba1^+$ in red) and plaques ($A\beta^+$ in green) for each corresponding area in 11-month-old rats.

(F) Representative binary images of EC microglia from 11- and 19-month-old rats per experimental group, obtained by confocal microscopy and cleaned with ImageJ software.

(G and H) Mean (G) circularity measured as $(4\pi \times \text{area}) \div \text{perimeter}^2$ and (H) microglial branch number per rat (both sexes combined). The effects of genotype, treatment, and age and the interactions between these factors were assessed by a three-way ANOVA followed by Fisher's LSD test. At 11 months old, $N = 4$ rats, and at 19 months old, $N = 10–11$ rats per experimental group. Data are presented as mean ± SEM; $^*p < 0.05$; $^{**}p < 0.01$; $^{***}p < 0.001$ and $\#p < 0.05$; $\#\#p < 0.01$; $\#\#\#p < 0.001$. Significant differences between 11 and 19 months per experimental group are denoted with "#."

Full statistical details are available in Table S6.

suggests distinct mechanisms of disease progression and resilience between sexes, underscoring the importance of accounting for sex in AD and brain resilience research, as it may lead to different therapeutic approaches depending on sex.

A change in PV expression in trained rats might contribute to the observed effects of cognitive stimulation, as a significant reduction of PV^+ immunoreactivity was clearly observed in the DG of trained rats (both WT and TG). A recent study reported that 9-month-old TgF344-AD rats exhibit neuronal loss in the EC and hippocampus, whereas at 12 months, a compensatory upregulation of GABAergic interneuronal markers was observed.[49] By 15 months, however, these animals show a robust loss of both excitatory and inhibitory neurons.[49] In our study, we did not observe such genotype-dependent differences, likely because our immunofluorescence analyses were performed at a later age (19 months), consistent with the age-dependent effects noted in Morrone et al.[49] GABAergic inhibitory interneurons play a key role in maintaining hippocampal excitation-inhibition balance, thereby synchronizing neuronal networks during memory encoding and retrieval. Age-related memory loss linked to hyperexcitability has been associated with reduced inhibitory input from the DG to the CA3.[50] Accordingly, loss of PV function has classically been associated with pathological states,[51] whereas restoration of PV-expressing interneuron function correlates with improved memory outcomes.[52,53] Nevertheless, the precise role of PV in memory processes and cognition in general, as well as in AD pathophysiology, remains incompletely understood and is still debated.[51,54]

Recent findings indicate that targeted suppression of PV^+ interneurons in the hippocampus can enhance CA3 output to CA1, increase slow gamma power, and improve memory consolidation and retrieval.[55] Furthermore, Donato and colleagues demonstrated that PV^+ interneuronal circuits exhibit bistable states, with environmental enrichment promoting a sustained, yet reversible, low-PV^+ network configuration that is associated with enhanced structural synaptic plasticity and improved NOR performance.[56] The authors observed that PV^+ neurons remained unchanged under different experimental conditions; rather, environmental experience altered PV expression levels.[56] Along this line, a study in a mouse model of autism suggested that reduced PV expression might represent an adaptive or compensatory mechanism aimed at restoring synaptic output.[57] In light of this evidence, while we cannot determine whether the reduction in PV immunoreactivity observed in our study reflects a loss of PV^+ interneurons or an activity-dependent downregulation of PV expression, we propose that it is more likely to represent functional modulation rather than neuronal death. Such modulation may contribute to the improved cognitive performance observed in trained animals. Future studies are required to disentangle these possibilities and clarify the mechanisms linking PV expression to cognitive resilience in aging and AD.

To investigate whether changes in fMRI connectivity reflect underlying molecular adaptations, we assessed synaptic and neuroplasticity-related protein levels in cortical lysates. Although the combined cortices may limit region-specific resolution, the lysates included areas with altered connectivity in fMRI, supporting a network-level interpretation. Thus, the observed restoration of PSD95 expression following cognitive stimulation, particularly in male TG rats, highlights the potential of behavioral interventions to preserve synaptic integrity. PSD95 is one of the most abundant postsynaptic proteins at excitatory synapses and plays a central role in regulating synaptic strength and plasticity through glutamatergic receptor trafficking, which is impaired in AD.[58] Reduced PSD95 expression has been consistently associated with Alzheimer's pathology and cognitive decline,[59–61] and its levels correlate with spatial memory performance.[62] VGLUT, a vesicular glutamate transporter, regulates presynaptic release probability and thereby influences synaptic activity.[63] Increased VGLUT expression has been proposed as a compensatory mechanism to counteract age-related postsynaptic receptor loss and maintain synaptic efficiency.[62] This may partially explain the elevated VGLUT levels observed in untrained TG females compared to WT animals, which coincided with preserved PSD95 expression. Interestingly, cognitive stimulation robustly decreased VGLUT expression to WT levels, suggesting that adaptive mechanisms of synaptic resilience may differ between males and females.

Phosphorylated S6 (p-RPS6), a key downstream effector of the mTOR pathway, regulates translational control and protein synthesis and is widely used as a marker of mTOR signaling activity.[64,65] The role of mTOR in AD remains debated: while hyperactivation has been implicated in amyloid and tau pathology,[66,67] reduced signaling may impair autophagic clearance of toxic proteins.[66,68] These discrepancies underscore the context-dependent role of mTOR in AD, with both overactivation and suppression producing deleterious outcomes depending on disease stage and cellular environment. To our knowledge, this is the first study to demonstrate alterations in mTOR signaling in TgF344-AD rats. We found a significant reduction of p-RPS6 in both male and female TG animals, which was partially restored by cognitive stimulation. In summary, beyond indicating normalization of synaptic protein expression, our results suggest that behavioral stimulation can directly engage molecular pathways critical for protein synthesis and plasticity, thereby supporting mechanisms of cognitive resilience in AD.

We also examined the neuroimmune environment. Microglia are critical for shaping synaptic plasticity, and therefore connectivity, contributing to CR.[69] Moreover, neuroinflammation is driven by chronically activated microglia, exacerbating neurodegeneration and cognitive decline in AD.[70,71] In agreement with previous studies,[72] our results further support the functional relevance of neuroinflammation in cognitive decline in TgF344-AD rats. For example, increased neuroinflammatory markers, including reactive microglia and elevated proinflammatory cytokines, correlate with impairments in spatial learning and memory in this rat model.[72] We observed that untrained TG rats had more circular and less branched microglia, indicative of a reactive phenotype, compared with WT counterparts. Conversely, long-term cognitive stimulation from early adulthood exerted a protective, anti-inflammatory effect at 11 months, reflected by an increased microglia-to-plaque ratio and a shift toward a homeostatic phenotype, morphologically characterized by highly ramified processes. Similar protective effects of environmental enrichment have been reported in response to human amyloid β-protein exposure, as shown by higher microglial density and a more ramified phenotype.[73] This anti-inflammatory effect of

cognitive stimulation could be essential for its protective potential, given the mechanistic link between chronic inflammation and cognitive impairment in neurodegenerative disorders.[4] Yet, by 19 months, microglial density decreased, and cells displayed a more ameboid phenotype in TG rats, independently of treatment. ''Inflammaging,'' the accumulated effect of chronic low-grade inflammation and microglial activation with aging,[74] may override the protective effect of cognitive training. Indeed, aging has been shown to exacerbate inflammation in TgF344-AD rats, resulting in hyperactive microglia by 18 months.[43] Such a dysmorphic phenotype may reflect a senescent state, in which microglia lose responsiveness to environmental cues,[75] indicating a limited temporal window during which cognitive stimulation can modulate neuroinflammatory processes.

Our study revealed clear sex differences in both the progression of AD-like pathology and the response to cognitive stimulation. Female untrained TG rats exhibited higher baseline expression levels of synaptic and neuroplasticity-related proteins (PSD95, TrkB, and VGLUT) than males, suggesting a degree of molecular resilience. In contrast, cognitive stimulation had a more pronounced protective effect in male TG rats, as evidenced by sustained functional connectivity, improved memory performance, and increased synaptic protein expression. Together, these results indicate sex-specific trajectories of disease and intervention response, likely driven by distinct underlying mechanisms of AD progression in males and females. Previous studies in the TgF344-AD rat model have shown that by 9 months of age, females display greater Aβ plaque burden, reduced glucose metabolism, and more pronounced anxiety-like and anhedonic behaviors, whereas males exhibit greater neuronal loss and more severe impairments in learning and memory.[13,15,16,76] These findings, together with ours, suggest that while females may initially display molecular resilience, they may ultimately experience a steeper functional decline once pathology is established. The DNMS task performance by TG females supports this hypothesis (Figure S1A). This pattern mirrors human data, in which women often exhibit a cognitive advantage during healthy aging but decline more rapidly following AD onset, indicating that early resilience may mask an underlying vulnerability that emerges with disease progression.[19]

Estrogen-mediated neuroprotection may partly explain the initial female advantage. However, since our study spanned from 3 to 19 months of age, females likely transitioned from regular cycling to acyclicity, with progressive declines in estradiol levels.[77] While fluctuations in ovarian hormones (estrous cycle) can influence microglial and synaptic outcomes,[78,79] such effects would vary over time and are unlikely to systematically impact long-term outcomes, particularly at 19 months when most females are post-reproductive. Future studies using ovariectomized models could further clarify the role of estrogen in sex-specific disease trajectories and intervention responses.

Overall, our findings highlight the need for sex-specific approaches in cognitive and pharmacological interventions, considering the differential timing and progression of pathology. Understanding how males and females differ in their molecular, functional, and behavioral responses to disease and treatment is critical for designing targeted strategies that optimize outcomes across sexes. Incorporating sex as a biological variable in preclinical AD research is essential to enhance translational relevance and guide more personalized therapeutic approaches.

In summary, our findings provide further insight into the progression of AD pathology in both female and male TG rats. We demonstrate that early periodic cognitive stimulation modifies the evolution of resting-state whole-brain functional connectomics and EC and hippocampus connectivity, acting as a compensatory mechanism against pathological aging. In males, this intervention notably preserves recognition memory, which may be attributed to reduced inhibitory function of hippocampal PV^+ interneurons, enhanced expression of plasticity-related proteins, and a less reactive microglial profile in the EC. At the same time, females showed a clear baseline advantage, with higher expression of synaptic markers and greater task engagement across genotypes, suggesting intrinsic molecular and functional resilience, particularly during the early stages of disease progression. However, this early advantage did not translate into stronger responses to cognitive stimulation, highlighting sex-specific trajectories in disease progression and intervention efficacy. Altogether, our study offers mechanistic insight into how early and sustained cognitive stimulation reshapes brain function in a sex-dependent manner, reinforcing its value as a preventive strategy in AD and underscoring the importance of considering sex-specific neurobiological mechanisms in the design of future interventions.

Limitations of the study

The main limitation of this study is the relatively small number of animals per experimental group, especially in rats sacrificed at 11 months. This constraint stems from the complexity of the longitudinal design, which included behavioral testing, MRI, brain sampling at two time points, and the inclusion of both sexes. Animal numbers were further constrained by the COVID-19 pandemic and cost considerations, particularly for DNMS training and MRI acquisitions. Despite this, the consistent trends across behavioral, imaging, and molecular domains strongly support our conclusion that cognitive stimulation exerts a protective effect. Moreover, our sex- and time-based analyses provide additional insight into disease progression and reinforce the importance of examining sex differences at the preclinical level for effective translational research.

While the behavioral data suggest a sex-specific benefit in trained TG males, our EC and hippocampus connectivity analyses did not reveal statistically significant sex differences (data not shown). This may reflect differences in sensitivity between behavioral and neuroimaging measures. Given the limited sample size, subgroup analyses by sex may have lacked the power to detect subtle effects. Thus, while behavioral patterns suggest sex specificity, seed-based connectivity findings likely reflect a general effect of cognitive stimulation in TG animals.

Species-specific differences should also be considered when translating rodent findings on CR to humans. Rodent models, including TgF344-AD rats, provide unique advantages for dissecting molecular, cellular, and network mechanisms of resilience, such as synaptic plasticity and microglial modulation, which are largely conserved across mammals.[80] These aspects likely reflect fundamental principles of CR that can inform human studies. However, the scope of CR in rodents is constrained by

differences in lifespan, the relative simplicity of behavioral repertoires, and neuroanatomical scaling, particularly the expansion of association cortices in humans that support higher order cognition.[81,82] Moreover, the environmental complexity and cognitive demands faced by humans are not fully recapitulated in laboratory conditions.[83,84] Therefore, while our results highlight mechanisms that may contribute to resilience, caution is warranted in extrapolating the magnitude and temporal dynamics of CR effects from rodents to humans.

RESOURCE AVAILABILITY

Lead contact

Further information and requests should be directed to and will be fulfilled by the lead contact, Guadalupe Soria (gsoria@ub.edu).

Materials availability

This study did not generate new unique reagents.

Data and code availability

- The datasets analyzed in the current study are available from the lead contact upon reasonable request.
- No original code was generated for this study.
- Any additional information required to reanalyze the data reported in this paper is available from the lead contact upon request.

ACKNOWLEDGMENTS

This work was partially funded by the Instituto de Salud Carlos III (ISCIII), PI18/00893, co-funded by the European Union "A way to make Europe," and grants PID2022-1363180B-I00 (G.S.), PID2019-107738RB-I00 (F.A.), PID2020-119236RB-I00 (C.M.), and CNS2023-144340 (G.S.) funded by MICIU/AEI/10.13039/501100011033/and by "ERDF A way of making Europe" and "European Union NextGenerationEU/PRTR." We are indebted to the Experimental MRI 7 T Unit of the Institut d'Investigacions Biòmediques August Pi I Sunyer. CIBER-BBN is an initiative financed by the Instituto de Salud Carlos III with assistance from the European Regional Development Fund. The project was also supported by the María de Maeztu Unit of Excellence (CEX2021-001159), Institute of Neurosciences of the University of Barcelona, Ministry of Science, Innovation, and Universities. Grants PREP2022-000586 (J.C.-P.) and PRE2022-102993 (E.A.-D.) were financed by MICIU/AEI/10.13039/501100011033 and by ESF+. The FI-2021 grant #FI-B-00378 was financed by the Agència de Gestió d'Ajuts Universitaris i de Recerca (AGAUR) (G.C.-C.). We thank Daniel Mayans, Luis Ferreiro, Carlota Domingo, Wenhui Zhou, Irene Sánchez-Domínguez, Noelia Castedo, and Xenia Sofianou for their assistance throughout the project.

AUTHOR CONTRIBUTIONS

X.L.-G., E.M.-M., R.T., L.M.-P., F.A., C.M., A.P.-G., and G.S. contributed to the conception and design of the study and designed the experiments. X.L.-G., J.C.-P., G.C.-C., E.A.-D., E.L.-B., C.G.-G., and G.S. performed all the experiments. F.V., J.C.-P., G.C.-C., and G.S. performed the statistical analysis. G.S. and A.P.-G. obtained financial support. J.C.-P. and G.S. wrote the manuscript. All authors reviewed and corrected the manuscript and agreed to the published version.

DECLARATION OF INTERESTS

The authors declare no competing interests.

DECLARATION OF GENERATIVE AI AND AI-ASSISTED TECHNOLOGIES IN THE WRITING PROCESS

During the preparation of this work, the authors used Paperpal to improve fluency in writing. After using this tool, the authors reviewed and edited the content as needed and take full responsibility for the content of the publication.

STAR★METHODS

Detailed methods are provided in the online version of this paper and include the following:

- KEY RESOURCES TABLE
- EXPERIMENTAL MODEL AND STUDY PARTICIPANT DETAILS
  - Animals and experimental design
- METHOD DETAILS
  - Training and delayed non-match to sample task
  - Novel object recognition test
  - Magnetic resonance imaging
  - Image processing and connectome definition
  - Connectome metrics
  - Seed-based analysis of the EC and the DG
  - Tissue preparation
  - Immunohistochemical studies
  - Immunofluorescence studies
  - Image acquisition and analysis
  - Western Blot analyses
- QUANTIFICATION AND STATISTICAL ANALYSIS

SUPPLEMENTAL INFORMATION

Supplemental information can be found online at https://doi.org/10.1016/j.isci.2025.114381.

Received: July 17, 2025
Revised: October 8, 2025
Accepted: December 4, 2025
Published: December 9, 2025

REFERENCES

1. Zhang, X.-X., Tian, Y., Wang, Z.-T., Ma, Y.-H., Tan, L., and Yu, J.-T. (2021). The Epidemiology of Alzheimer's Disease Modifiable Risk Factors and Prevention. J. Prev. Alzheimers Dis. *8*, 313–321. https://doi.org/10.14283/jpad.2021.15.
2. Carlson, M.C., Saczynski, J.S., Rebok, G.W., Seeman, T., Glass, T.A., McGill, S., Tielsch, J., Frick, K.D., Hill, J., and Fried, L.P. (2008). Exploring the Effects of an "Everyday" Activity Program on Executive Function and Memory in Older Adults: Experience Corps®. Gerontol. *48*, 793–801. https://doi.org/10.1093/geront/48.6.793.
3. Park, D.C., Lodi-Smith, J., Drew, L., Haber, S., Hebrank, A., Bischof, G.N., and Aamodt, W. (2014). The Impact of Sustained Engagement on Cognitive Function in Older Adults: The Synapse Project. Psychol. Sci. *25*, 103–112. https://doi.org/10.1177/0956797613499592.
4. Phillips, C. (2017). Lifestyle Modulators of Neuroplasticity: How Physical Activity, Mental Engagement, and Diet Promote Cognitive Health during Aging. Neural Plast. *2017*, e3589271. https://doi.org/10.1155/2017/3589271.
5. Stern, Y. (2012). Cognitive reserve in ageing and Alzheimer's disease. Lancet Neurol. *11*, 1006–1012. https://doi.org/10.1016/S1474-4422(12)70191-6.
6. Stern, Y., Albert, M., Barnes, C.A., Cabeza, R., Pascual-Leone, A., and Rapp, P.R. (2023). A framework for concepts of reserve and resilience in aging. Neurobiol. Aging *124*, 100–103. https://doi.org/10.1016/j.neurobiolaging.2022.10.015.

7. Bartrés-Faz, D., González-Escamilla, G., Vaqué-Alcázar, L., Abellaneda-Pérez, K., Valls-Pedret, C., Ros, E., and Grothe, M.J. (2019). Characterizing the Molecular Architecture of Cortical Regions Associated with High Educational Attainment in Older Individuals. J. Neurosci. *39*, 4566–4575. https://doi.org/10.1523/JNEUROSCI.2370-18.2019.

8. Sundermann, E.E., Maki, P.M., Reddy, S., Bondi, M.W., Biegon, A., and Alzheimer's Disease Neuroimaging Initiative. (2020). Women's higher brain metabolic rate compensates for early Alzheimer's pathology. Alzheimer's Dement. *12*, e12121. https://doi.org/10.1002/dad2.12121.

9. Caldwell, J.Z.K., and Isenberg, N. (2023). The aging brain: risk factors and interventions for long term brain health in women. Curr. Opin. Obstet. Gynecol. *35*, 169–175. https://doi.org/10.1097/GCO.0000000000000849.

10. Vila-Castelar, C., Guzmán-Vélez, E., Pardilla-Delgado, E., Buckley, R.F., Bocanegra, Y., Baena, A., Fox-Fuller, J.T., Tirado, V., Muñoz, C., Giraldo, M., et al. (2020). Examining Sex Differences in Markers of Cognition and Neurodegeneration in Autosomal Dominant Alzheimer's Disease: Preliminary Findings from the Colombian Alzheimer's Prevention Initiative Biomarker Study. J. Alzheimer's Dis. *77*, 1743–1753. https://doi.org/10.3233/JAD-200723.

11. Zissimopoulos, J., Crimmins, E., and St.Clair, P. (2015). The Value of Delaying Alzheimer's Disease Onset. Forum Health Econ. Policy *18*, 25–39. https://doi.org/10.1515/fhep-2014-0013.

12. Cohen, R.M., Rezai-Zadeh, K., Weitz, T.M., Rentsendorj, A., Gate, D., Spivak, I., Bholat, Y., Vasilevko, V., Glabe, C.G., Breunig, J.J., et al. (2013). A Transgenic Alzheimer Rat with Plaques, Tau Pathology, Behavioral Impairment, Oligomeric Aβ, and Frank Neuronal Loss. J. Neurosci. *33*, 6245–6256. https://doi.org/10.1523/JNEUROSCI.3672-12.2013.

13. Chaudry, O., Ndukwe, K., Xie, L., Figueiredo-Pereira, M., Serrano, P., and Rockwell, P. (2022). Females exhibit higher GluA2 levels and outperform males in active place avoidance despite increased amyloid plaques in TgF344-Alzheimer's rats. Sci. Rep. *12*, 19129. https://doi.org/10.1038/s41598-022-23801-w.

14. Ndukwe, K., Serrano, P.A., Rockwell, P., Xie, L., and Figueiredo-Pereira, M.E. (2025). Brain-penetrant histone deacetylase inhibitor RG2833 improves spatial memory in females of an Alzheimer's disease rat model. J. Alzheimer's Dis. *104*, 173–190. https://doi.org/10.1177/13872877251314777.

15. Srivastava, H., Lasher, A.T., Nagarajan, A., and Sun, L.Y. (2023). Sexual dimorphism in the peripheral metabolic homeostasis and behavior in the TgF344-AD rat model of Alzheimer's disease. Aging Cell *22*, e13854. https://doi.org/10.1111/acel.13854.

16. Hernandez, C.M., McCuiston, M.A., Davis, K., Halls, Y., Carcamo Dal Zotto, J.P., Jackson, N.L., Dobrunz, L.E., King, P.H., and McMahon, L.L. (2024). In a circuit necessary for cognition and emotional affect, Alzheimer's-like pathology associates with neuroinflammation, cognitive and motivational deficits in the young adult TgF344-AD rat. Brain Behav. Immun. Health *39*, 100798. https://doi.org/10.1016/j.bbih.2024.100798.

17. Ostlund, S.B., Chen, G., Kosheleff, A., Lueptow, L.M., Zhuravka, I., Frautschy, S.A., Lam, H.A., and Maidment, N.T. (2025). Early emergence of motivational and hedonic feeding deficits in the TgF344-AD rat model of Alzheimer's disease. Front. Aging Neurosci. *17*, 1572956. https://doi.org/10.3389/fnagi.2025.1572956.

18. Rosende-Roca, M., García-Gutiérrez, F., Cantero-Fortiz, Y., Alegret, M., Pytel, V., Cañabate, P., González-Pérez, A., de Rojas, I., Vargas, L., Tartari, J.P., et al. (2025). Exploring sex differences in Alzheimer's disease: a comprehensive analysis of a large patient cohort from a memory unit. Alzheimers Res. Ther. *17*, 27. https://doi.org/10.1186/s13195-024-01656-9.

19. Arenaza-Urquijo, E.M., Boyle, R., Casaletto, K., Anstey, K.J., Vila-Castelar, C., Colverson, A., Palpatzis, E., Eissman, J.M., Kheng Siang Ng, T., Raghavan, S., et al. (2024). Sex and gender differences in cognitive resilience to aging and Alzheimer's disease. Alzheimer's Dement. *20*, 5695–5719. https://doi.org/10.1002/alz.13844.

20. Muñoz-Moreno, E., Tudela, R., López-Gil, X., and Soria, G. (2018). Early brain connectivity alterations and cognitive impairment in a rat model of Alzheimer's disease. Alzheimers Res. Ther. *10*, 16. https://doi.org/10.1186/s13195-018-0346-2.

21. Muñoz-Moreno, E., Tudela, R., López-Gil, X., and Soria, G. (2020). Brain connectivity during Alzheimer's disease progression and its cognitive impact in a transgenic rat model. Netw. Neurosci. *4*, 397–415. https://doi.org/10.1162/netn_a_00126.

22. Tudela, R., Muñoz-Moreno, E., Sala-Llonch, R., López-Gil, X., and Soria, G. (2019). Resting State Networks in the TgF344-AD Rat Model of Alzheimer's Disease Are Altered From Early Stages. Front. Aging Neurosci. *11*. https://doi.org/10.3389/fnagi.2019.00213.

23. Rodriguez, J.S., and Paule, M.G. (2009). Working Memory Delayed Response Tasks in Monkeys. In Methods of Behavior Analysis in Neuroscience Frontiers in Neuroscience, J.J. Buccafusco, ed. (CRC Press/Taylor & Francis).

24. Antunes, M., and Biala, G. (2012). The novel object recognition memory: neurobiology, test procedure, and its modifications. Cogn. Process. *13*, 93–110. https://doi.org/10.1007/s10339-011-0430-z.

25. Takeuchi, H., Taki, Y., and Kawashima, R. (2010). Effects of Working Memory Training on Cognitive Functions and Neural Systems. Rev. Neurosci. *21*, 427–449. https://doi.org/10.1515/REVNEURO.2010.21.6.427.

26. Martinez-Coria, H., Yeung, S.T., Ager, R.R., Rodriguez-Ortiz, C.J., Baglietto-Vargas, D., and LaFerla, F.M. (2015). Repeated cognitive stimulation alleviates memory impairments in an Alzheimer's disease mouse model. Brain Res. Bull. *117*, 10–15. https://doi.org/10.1016/j.brainresbull.2015.07.001.

27. Burnyasheva, A.O., Kozlova, T.A., Stefanova, N.A., Kolosova, N.G., and Rudnitskaya, E.A. (2020). Cognitive Training as a Potential Activator of Hippocampal Neurogenesis in the Rat Model of Sporadic Alzheimer's Disease. Int. J. Mol. Sci. *21*, 6986. https://doi.org/10.3390/ijms21196986.

28. de Paula França Resende, E., Lara, V.P., Santiago, A.L.C., Friedlaender, C.V., Rosen, H.J., Brown, J.A., Cobigo, Y., Silva, L.L.G., Cruz de Souza, L., Rincon, L., et al. (2024). Health literacy, but not memory, is associated with hippocampal connectivity in adults with low levels of formal education. Alzheimers Dement Diagn. Assess. Dis. Monit. *16*, e12634. https://doi.org/10.1002/dad2.12634.

29. Bengoetxea, X., Rodriguez-Perdigon, M., and Ramirez, M.J. (2015). Object recognition test for studying cognitive impairments in animal models of Alzheimer's disease. Front. Biosci. *7*, 10–29. https://doi.org/10.2741/S421.

30. Leitch, B. (2024). Parvalbumin Interneuron Dysfunction in Neurological Disorders: Focus on Epilepsy and Alzheimer's Disease. Int. J. Mol. Sci. *25*, 5549. https://doi.org/10.3390/ijms25105549.

31. Zhao, R., Hu, W., Tsai, J., Li, W., and Gan, W.-B. (2017). Microglia limit the expansion of β-amyloid plaques in a mouse model of Alzheimer's disease. Mol. Neurodegener. *12*, 47. https://doi.org/10.1186/s13024-017-0188-6.

32. Carrier, M., Robert, M.-È., González Ibáñez, F., Desjardins, M., and Tremblay, M.-È. (2020). Imaging the Neuroimmune Dynamics Across Space and Time. Front. Neurosci. *14*. https://doi.org/10.3389/fnins.2020.00903.

33. Navakkode, S., and Kennedy, B.K. (2024). Neural ageing and synaptic plasticity: prioritizing brain health in healthy longevity. Front. Aging Neurosci. *16*, 1428244. https://doi.org/10.3389/fnagi.2024.1428244.

34. Ewers, M., Luan, Y., Frontzkowski, L., Neitzel, J., Rubinski, A., Dichgans, M., Hassenstab, J., Gordon, B.A., Chhatwal, J.P., Levin, J., et al. (2021). Segregation of functional networks is associated with cognitive resilience in Alzheimer's disease. Brain *144*, 2176–2185. https://doi.org/10.1093/brain/awab112.

35. Liu, Y., Yu, C., Zhang, X., Liu, J., Duan, Y., Alexander-Bloch, A.F., Liu, B., Jiang, T., and Bullmore, E. (2014). Impaired Long Distance Functional

Connectivity and Weighted Network Architecture in Alzheimer's Disease. Cereb. Cortex *24*, 1422–1435. https://doi.org/10.1093/cercor/bhs410.

36. Franzmeier, N., Caballero, M.Á.A., Taylor, A.N.W., Simon-Vermot, L., Buerger, K., Ertl-Wagner, B., Mueller, C., Catak, C., Janowitz, D., Baykara, E., et al. (2017). Resting-state global functional connectivity as a biomarker of cognitive reserve in mild cognitive impairment. Brain Imaging Behav. *11*, 368–382. https://doi.org/10.1007/s11682-016-9599-1.

37. Wang, S., Wang, Y., Xu, F.H., Tian, X., Fredericks, C.A., Shen, L., Zhao, Y., and Alzheimer's Disease Neuroimaging Initiative. (2024). Sex-specific topological structure associated with dementia via latent space estimation. Alzheimer's Dement. *20*, 8387–8401. https://doi.org/10.1002/alz.14266.

38. van den Berg, M., Adhikari, M.H., Verschuuren, M., Pintelon, I., Vasilkovska, T., Van Audekerke, J., Missault, S., Heymans, L., Ponsaerts, P., De Vos, W.H., et al. (2022). Altered basal forebrain function during whole-brain network activity at pre- and early-plaque stages of Alzheimer's disease in TgF344-AD rats. Alzheimers Res. Ther. *14*, 148. https://doi.org/10.1186/s13195-022-01089-2.

39. De Waegenaere, S., van den Berg, M., Keliris, G.A., Adhikari, M.H., and Verhoye, M. (2024). Early altered directionality of resting brain network state transitions in the TgF344-AD rat model of Alzheimer's disease. Front. Hum. Neurosci. *18*, 1379923. https://doi.org/10.3389/fnhum.2024.1379923.

40. Anckaerts, C., Blockx, I., Summer, P., Michael, J., Hamaide, J., Kreutzer, C., Boutin, H., Couillard-Després, S., Verhoye, M., and Van der Linden, A. (2019). Early functional connectivity deficits and progressive microstructural alterations in the TgF344-AD rat model of Alzheimer's Disease: A longitudinal MRI study. Neurobiol. Dis. *124*, 93–107. https://doi.org/10.1016/j.nbd.2018.11.010.

41. Pagani, M., Gutierrez-Barragan, D., de Guzman, A.E., Xu, T., and Gozzi, A. (2023). Mapping and comparing fMRI connectivity networks across species. Commun. Biol. *6*, 1238. https://doi.org/10.1038/s42003-023-05629-w.

42. Bizon, J.L., LaSarge, C.L., Montgomery, K.S., McDermott, A.N., Setlow, B., and Griffith, W.H. (2009). Spatial reference and working memory across the lifespan of male Fischer 344 rats. Neurobiol. Aging *30*, 646–655. https://doi.org/10.1016/j.neurobiolaging.2007.08.004.

43. Chaney, A.M., Lopez-Picon, F.R., Serrière, S., Wang, R., Bochicchio, D., Webb, S.D., Vandesquille, M., Harte, M.K., Georgiadou, C., Lawrence, C., et al. (2021). Prodromal neuroinflammatory, cholinergic and metabolite dysfunction detected by PET and MRS in the TgF344-AD transgenic rat model of AD: a collaborative multi-modal study. Theranostics *11*, 6644–6667. https://doi.org/10.7150/thno.56059.

44. Galloway, C.R., Ravipati, K., Singh, S., Lebois, E.P., Cohen, R.M., Levey, A.I., and Manns, J.R. (2018). Hippocampal place cell dysfunction and the effects of muscarinic M1 receptor agonism in a rat model of Alzheimer's disease. Hippocampus *28*, 568–585. https://doi.org/10.1002/hipo.22961.

45. Bernaud, V.E., Bulen, H.L., Peña, V.L., Koebele, S.V., Northup-Smith, S.N., Manzo, A.A., Valenzuela Sanchez, M., Opachich, Z., Ruhland, A.M., and Bimonte-Nelson, H.A. (2022). Task-dependent learning and memory deficits in the TgF344-AD rat model of Alzheimer's disease: three key timepoints through middle-age in females. Sci. Rep. *12*, 14596. https://doi.org/10.1038/s41598-022-18415-1.

46. Zarezadehmehrizi, A., Hong, J., Lee, J., Rajabi, H., Gharakhanlu, R., Naghdi, N., Azimi, M., and Park, Y. (2021). Exercise training ameliorates cognitive dysfunction in amyloid beta-injected rat model: possible mechanisms of Angiostatin/VEGF signaling. Metab. Brain Dis. *36*, 2263–2271. https://doi.org/10.1007/s11011-021-00751-2.

47. Yang, L., Wu, C., Li, Y., Dong, Y., Wu, C.Y.-C., Lee, R.H.-C., Brann, D.W., Lin, H.W., and Zhang, Q. (2022). Long-term exercise pre-training attenuates Alzheimer's disease–related pathology in a transgenic rat model of Alzheimer's disease. GeroScience *44*, 1457–1477. https://doi.org/10.1007/s11357-022-00534-2.

48. Hall, S.E., White, Z.J., Rohn, T.T., Sudasinghe, K.H., and Young, M.E. (2025). Exercise Improves Alzheimer's Disease Phenotype in the TgF344-AD Rat, a Behavioral Time Course Study of Males and Females. Brain Sci. *15*, 631. https://doi.org/10.3390/brainsci15060631.

49. Morrone, C.D., Lai, A.Y., Bishay, J., Hill, M.E., and McLaurin, J. (2022). Parvalbumin neuroplasticity compensates for somatostatin impairment, maintaining cognitive function in Alzheimer's disease. Transl. Neurodegener. *11*, 26. https://doi.org/10.1186/s40035-022-00300-6.

50. Hernández-Frausto, M., and Vivar, C. (2024). Entorhinal cortex–hippocampal circuit connectivity in health and disease. Front. Hum. Neurosci. *18*. https://doi.org/10.3389/fnhum.2024.1448791.

51. Ruden, J.B., Dugan, L.L., and Konradi, C. (2021). Parvalbumin interneuron vulnerability and brain disorders. Neuropsychopharmacology *46*, 279–287. https://doi.org/10.1038/s41386-020-0778-9.

52. Serra, F.T., Araujo, B.H.S., Placencia, E.V.D., Henrique, J.S., Dona, F., Torres, L.B., Fernandes, M.J.d.S., Arida, R.M., and Gomes da Silva, S. (2020). Enriched environment and exercise effects on parvalbumin expression and distribution in the hippocampal formation of developing rats. Brain Res. Bull. *160*, 85–90. https://doi.org/10.1016/j.brainresbull.2020.03.021.

53. Hijazi, S., Heistek, T.S., Scheltens, P., Neumann, U., Shimshek, D.R., Mansvelder, H.D., Smit, A.B., and van Kesteren, R.E. (2020). Early restoration of parvalbumin interneuron activity prevents memory loss and network hyperexcitability in a mouse model of Alzheimer's disease. Mol. Psychiatry *25*, 3380–3398. https://doi.org/10.1038/s41380-019-0483-4.

54. Merino-Serrais, P., Plaza-Alonso, S., Tapia-Gonzalez, S., León-Espinosa, G., and DeFelipe, J. (2025). Parvalbumin interneurons in the hippocampal formation of individuals with Alzheimer's disease: a neuropathological study of abnormal phosphorylated tau in neurons. Front. Neuroanat. *19*, 1571514. https://doi.org/10.3389/fnana.2025.1571514.

55. Jones, E.A.A., Rao, A., Zilberter, M., Djukic, B., Bant, J.S., Gillespie, A.K., Koutsodendris, N., Nelson, M., Yoon, S.Y., Huang, K., et al. (2021). Dentate gyrus and CA3 GABAergic interneurons bidirectionally modulate signatures of internal and external drive to CA1. Cell Rep. *37*, 110159. https://doi.org/10.1016/j.celrep.2021.110159.

56. Donato, F., Rompani, S.B., and Caroni, P. (2013). Parvalbumin-expressing basket-cell network plasticity induced by experience regulates adult learning. Nature *504*, 272–276. https://doi.org/10.1038/nature12866.

57. Filice, F., Vörckel, K.J., Sungur, A.Ö., Wöhr, M., and Schwaller, B. (2016). Reduction in parvalbumin expression not loss of the parvalbumin-expressing GABA interneuron subpopulation in genetic parvalbumin and shank mouse models of autism. Mol. Brain *9*, 10. https://doi.org/10.1186/s13041-016-0192-8.

58. Hyman, B.T., and Trojanowski, J.Q. (1997). Editorial on Consensus Recommendations for the Postmortem Diagnosis of Alzheimer Disease from the National Institute on Aging and the Reagan Institute Working Group on Diagnostic Criteria for the Neuropathological Assessment of Alzheimer Disease. J. Neuropathol. Exp. Neurol. *56*, 1095–1097. https://doi.org/10.1097/00005072-199710000-00002.

59. Savioz, A., Leuba, G., and Vallet, P.G. (2014). A framework to understand the variations of PSD-95 expression in brain aging and in Alzheimer's disease. Ageing Res. Rev. *18*, 86–94. https://doi.org/10.1016/j.arr.2014.09.004.

60. Serrano, G.E., Walker, J., Nelson, C., Glass, M., Arce, R., Intorcia, A., Cline, M.P., Nabaty, N., Acuña, A., Huppert Steed, A., et al. (2024). Correlation of Presynaptic and Postsynaptic Proteins with Pathology in Alzheimer's Disease. Int. J. Mol. Sci. *25*, 3130. https://doi.org/10.3390/ijms25063130.

61. P, A.,H., Basavaraju, N., Chandran, M., Jaleel, A., Bennett, D.A., and Kommaddi, R.P. (2024). Mitigation of synaptic and memory impairments via F-actin stabilization in Alzheimer's disease. Alzheimers Res. Ther. *16*, 200. https://doi.org/10.1186/s13195-024-01558-w.

62. Ménard, C., Quirion, R., Vigneault, E., Bouchard, S., Ferland, G., El Mestikawy, S., and Gaudreau, P. (2015). Glutamate presynaptic vesicular transporter and postsynaptic receptor levels correlate with spatial memory status in aging rat models. Neurobiol. Aging *36*, 1471–1482. https://doi.org/10.1016/j.neurobiolaging.2014.11.013.

63. Herman, M.A., Ackermann, F., Trimbuch, T., and Rosenmund, C. (2014). Vesicular Glutamate Transporter Expression Level Affects Synaptic Vesicle Release Probability at Hippocampal Synapses in Culture. J. Neurosci. *34*, 11781–11791. https://doi.org/10.1523/JNEUROSCI.1444-14.2014.

64. Leontieva, O.V., Paszkiewicz, G.M., and Blagosklonny, M.V. (2012). Mechanistic or mammalian target of rapamycin (mTOR) may determine robustness in young male mice at the cost of accelerated aging. Aging *4*, 899–916. https://doi.org/10.18632/aging.100528.

65. Morgan-Warren, P.J., Berry, M., Ahmed, Z., Scott, R.A.H., and Logan, A. (2013). Exploiting mTOR Signaling: A Novel Translatable Treatment Strategy for Traumatic Optic Neuropathy? Investig. Ophthalmol. Vis. Sci. *54*, 6903–6916. https://doi.org/10.1167/iovs.13-12803.

66. Caccamo, A., Majumder, S., Richardson, A., Strong, R., and Oddo, S. (2010). Molecular Interplay between Mammalian Target of Rapamycin (mTOR), Amyloid-β, and Tau: EFFECTS ON COGNITIVE IMPAIRMENTS. J. Biol. Chem. *285*, 13107–13120. https://doi.org/10.1074/jbc.M110.100420.

67. Querfurth, H., and Lee, H.-K. (2021). Mammalian/mechanistic target of rapamycin (mTOR) complexes in neurodegeneration. Mol. Neurodegener. *16*, 44. https://doi.org/10.1186/s13024-021-00428-5.

68. Ahmad, F., Singh, K., Das, D., Gowaikar, R., Shaw, E., Ramachandran, A., Rupanagudi, K.V., Kommaddi, R.P., Bennett, D.A., and Ravindranath, V. (2017). Reactive Oxygen Species-Mediated Loss of Synaptic Akt1 Signaling Leads to Deficient Activity-Dependent Protein Translation Early in Alzheimer's Disease. Antioxid. Redox Signal. *27*, 1269–1280. https://doi.org/10.1089/ars.2016.6860.

69. Verkhratsky, A., and Zorec, R. (2024). Neuroglia in cognitive reserve. Mol. Psych. *29*, 3962–3967. https://doi.org/10.1038/s41380-024-02644-z.

70. Ownby, R.L. (2010). Neuroinflammation and Cognitive Aging. Curr. Psychiatry Rep. *12*, 39–45. https://doi.org/10.1007/s11920-009-0082-1.

71. Cai, Z., Hussain, M.D., and Yan, L.-J. (2014). Microglia, neuroinflammation, and beta-amyloid protein in Alzheimer's disease. Int. J. Neurosci. *124*, 307–321. https://doi.org/10.3109/00207454.2013.833510.

72. Bac, B., Hicheri, C., Weiss, C., Buell, A., Vilcek, N., Spaeni, C., Geula, C., Savas, J.N., and Disterhoft, J.F. (2023). The TgF344-AD rat: behavioral and proteomic changes associated with aging and protein expression in a transgenic rat model of Alzheimer's disease. Neurobiol. Aging *123*, 98–110. https://doi.org/10.1016/j.neurobiolaging.2022.12.015.

73. Xu, H., Gelyana, E., Rajsombath, M., Yang, T., Li, S., and Selkoe, D. (2016). Environmental Enrichment Potently Prevents Microglia-Mediated Neuroinflammation by Human Amyloid β-Protein Oligomers. J. Neurosci. *36*, 9041–9056. https://doi.org/10.1523/JNEUROSCI.1023-16.2016.

74. Hanslik, K.L., and Ulland, T.K. (2020). The Role of Microglia and the Nlrp3 Inflammasome in Alzheimer's Disease. Front. Neurol. *11*, 570711. https://doi.org/10.3389/fneur.2020.570711.

75. Harry, G.J. (2013). Microglia during development and aging. Pharmacol. Ther. *139*, 313–326. https://doi.org/10.1016/j.pharmthera.2013.04.013.

76. Lopez, D.C., White, Z.J., and Hall, S.E. (2024). Anxiety in Alzheimer's disease rats is independent of memory and impacted by genotype, age, sex, and exercise. Alzheimer's Dement. *20*, 3543–3550. https://doi.org/10.1002/alz.13813.

77. Morrison, J.H., Brinton, R.D., Schmidt, P.J., and Gore, A.C. (2006). Estrogen, Menopause, and the Aging Brain: How Basic Neuroscience Can Inform Hormone Therapy in Women. J. Neurosci. *26*, 10332–10348. https://doi.org/10.1523/JNEUROSCI.3369-06.2006.

78. Frick, K.M. (2009). Estrogens and age-related memory decline in rodents: What have we learned and where do we go from here? Horm. Beyond Behav. *55*, 2–23. https://doi.org/10.1016/j.yhbeh.2008.08.015.

79. Baudin, J., Antolín, A., Fernández-Arroyo, S., Del Pino, A., Mulero, F., Puiggròs, F., Arola, L., and Caimari, A. (2025). Impact of the natural female reproductive aging on the rat serum lipidome. Clin. Sci. *139*, 957–977. https://doi.org/10.1042/CS20255841.

80. de Vries, L.E., Huitinga, I., Kessels, H.W., Swaab, D.F., and Verhaagen, J. (2024). The concept of resilience to Alzheimer's Disease: current definitions and cellular and molecular mechanisms. Mol. Neurodegener. *19*, 33. https://doi.org/10.1186/s13024-024-00719-7.

81. Herculano-Houzel, S. (2017). Numbers of neurons as biological correlates of cognitive capability. Curr. Opin. Behav. Sci. *16*, 1–7. https://doi.org/10.1016/j.cobeha.2017.02.004.

82. Galakhova, A.A., Hunt, S., Wilbers, R., Heyer, D.B., de Kock, C.P.J., Mansvelder, H.D., and Goriounova, N.A. (2022). Evolution of cortical neurons supporting human cognition. Trends Cogn. Sci. *26*, 909–922. https://doi.org/10.1016/j.tics.2022.08.012.

83. Robbins, T.W. (2015). From Rodent Behavioral Models to Human Disorders. In Translational Neuroscience: Toward New Therapies, K. Nikolich and S.E. Hyman, eds. (MIT Press).

84. Gattas, S., Collett, H.A., Huff, A.E., Creighton, S.D., Weber, S.E., Buckhalter, S.S., Manning, S.A., Ryait, H.S., McNaughton, B.L., and Winters, B.D. (2022). A rodent obstacle course procedure controls delivery of enrichment and enhances complex cognitive functions. Npj Sci. Learn. *7*, 21. https://doi.org/10.1038/s41539-022-00134-x.

85. Avants, B., Tustison, N.J., and Song, G. (2009). Advanced Normalization Tools: V1.0. Insight J. https://doi.org/10.54294/uvnhin.

86. Barrière, D.A., Magalhães, R., Novais, A., Marques, P., Selingue, E., Geffroy, F., Marques, F., Cerqueira, J., Sousa, J.C., Boumezbeur, F., et al. (2019). The SIGMA rat brain templates and atlases for multimodal MRI data analysis and visualization. Nat. Commun. *10*, 5699. https://doi.org/10.1038/s41467-019-13575-7.

87. Tournier, J.-D., Smith, R., Raffelt, D., Tabbara, R., Dhollander, T., Pietsch, M., Christiaens, D., Jeurissen, B., Yeh, C.-H., and Connelly, A. (2019). *MRtrix3*: A fast, flexible and open software framework for medical image processing and visualisation. Neuroimage *202*, 116137. https://doi.org/10.1016/j.neuroimage.2019.116137.

88. contributors, N., Chamma, A., Frau-Pascual, A., Rothberg, A., Abadie, A., Abraham, A., Gramfort, A., Savio, A., Cionca, A., Sayal, A., et al. (2025). Nilearn (Zenodo). https://doi.org/10.5281/zenodo.17043133.

89. Power, J.D., Plitt, M., Laumann, T.O., and Martin, A. (2017). Sources and implications of whole-brain fMRI signals in humans. Neuroimage *146*, 609–625. https://doi.org/10.1016/j.neuroimage.2016.09.038.

90. Rubinov, M., and Sporns, O. (2010). Complex network measures of brain connectivity: Uses and interpretations. Neuroimage *52*, 1059–1069. https://doi.org/10.1016/j.neuroimage.2009.10.003.

91. Sanz-Arigita, E.J., Schoonheim, M.M., Damoiseaux, J.S., Rombouts, S.A.R.B., Maris, E., Barkhof, F., Scheltens, P., and Stam, C.J. (2010). Loss of 'Small-World' Networks in Alzheimer's Disease: Graph Analysis of fMRI Resting-State Functional Connectivity. PLoS One *5*, e13788. https://doi.org/10.1371/journal.pone.0013788.

92. Daianu, M., Jahanshad, N., Nir, T.M., Toga, A.W., Jack, C.R., Weiner, M.W., Thompson, for the Alzheimer's Disease Neuroimaging Initiative, and Alzheimer's Disease Neuroimaging Initiative. (2013). Breakdown of Brain Connectivity Between Normal Aging and Alzheimer's Disease: A Structural k-Core Network Analysis. Brain Connect. *3*, 407–422. https://doi.org/10.1089/brain.2012.0137.

93. Brier, M.R., Thomas, J.B., and Ances, B.M. (2014). Network Dysfunction in Alzheimer's Disease: Refining the Disconnection Hypothesis. Brain Connect. *4*, 299–311. https://doi.org/10.1089/brain.2014.0236.

94. Fischer, F.U., Wolf, D., Scheurich, A., Fellgiebel, A., and Alzheimer's Disease Neuroimaging Initiative. (2015). Altered whole-brain white matter

networks in preclinical Alzheimer's disease. Neuroimage. Clin. *8*, 660–666. https://doi.org/10.1016/j.nicl.2015.06.007.

95. Smitha, K.A., Akhil Raja, K., Arun, K.M., Rajesh, P.G., Thomas, B., Kapilamoorthy, T.R., and Kesavadas, C. (2017). Resting state fMRI: A review on methods in resting state connectivity analysis and resting state networks. Neuroradiol. J. *30*, 305–317. https://doi.org/10.1177/1971400917697342.
96. Winkler, A.M., Ridgway, G.R., Webster, M.A., Smith, S.M., and Nichols, T.E. (2014). Permutation inference for the general linear model. Neuroimage *92*, 381–397. https://doi.org/10.1016/j.neuroimage.2014.01.060.
97. Smith, S.M., and Nichols, T.E. (2009). Threshold-free cluster enhancement: Addressing problems of smoothing, threshold dependence and localisation in cluster inference. Neuroimage *44*, 83–98. https://doi.org/10.1016/j.neuroimage.2008.03.061.
98. Yushkevich, P.A., Piven, J., Hazlett, H.C., Smith, R.G., Ho, S., Gee, J.C., and Gerig, G. (2006). User-guided 3D active contour segmentation of anatomical structures: Significantly improved efficiency and reliability. Neuroimage *31*, 1116–1128. https://doi.org/10.1016/j.neuroimage.2006.01.015.
99. Paxinos, G., and Watson, C. (2013). The Rat Brain in Stereotaxic Coordinates (Academic Press).
100. Thacker, J.S., Andersen, D., Liang, S., Zieniewicz, N., Trivino-Paredes, J.S., Nahirney, P.C., and Christie, B.R. (2021). Unlocking the brain: A new method for Western blot protein detection from fixed brain tissue. J. Neurosci. Methods *348*, 108995. https://doi.org/10.1016/j.jneumeth.2020.108995.

STAR★METHODS

KEY RESOURCES TABLE

REAGENT or RESOURCE	SOURCE	IDENTIFIER
Antibodies		
Rabbit monoclonal anti-NeuN	Abcam	Cat#177487; RRID:AB_2532109
Mouse monoclonal anti-Beta-Amyloid	Dako	Cat# M0872; RRID:AB_2056966
Goat HRP-linked anti-rabbit	Cell Signaling Technology	Cat#7074; Lot:33; RRID:AB_2099233
Goat HRP-linked anti-mouse	Thermo Fisher Scientific	Cat#32430; Lot: YL383646; RRID:AB_1185566
Rabbit polyclonal anti-Iba1	Wako	Cat#019–19741; Lot: WDE1198; RRID:AB_839504
Rabbit polyclonal anti-parvalbumin	Proteintech	Cat #29312-1-AP; RRID:AB_2918280
Goat anti-mouse Alexa Fluor 488	Thermo Fisher Scientific	Cat#A31620; Lot: 2415939
Donkey anti-rabbit Alexa Fluor 546	Thermo Fisher Scientific	Cat#A10040; Lot: 2273718; RRID:AB_2534016
Fluoroshield with DAPI	Sigma-Aldrich	Cat#F6057; Lot: 0000405985
Mouse monoclonal anti-PSD-95	Thermo Fisher Scientific	Cat#MA1-045; RRID:AB_325399
Rabbit polyclonal anti-VGLUT1	Synaptic Systems	Cat#135303; RRID:AB_887875
Rabbit monoclonal anti-*p*-RPS6 (Ser235/236)	Cell Signaling Technology	Cat#4858; RRID:AB_916156
Mouse monoclonal anti-RPS6	Cell Signaling Technology	Cat#2317; RRID:AB_2238583
Mouse monoclonal anti-TrkB	BD Biosciences	Cat#610102; RRID:AB_397508
Goat HRP-linked anti-mouse	Thermo Fisher Scientific	Cat#31430; RRID:AB_228307
Goat HRP-linked anti-rabbit	Thermo Fisher Scientific	Cat#31460; RRID:AB_228341
Critical commercial assays		
Protein Assay kit	Bio-Rad	Cat#5000112
Experimental models: Organisms/strains		
Rat: TgF344-AD: Rat: F344-Tg(Prp-APP,Prp-PS1)19/Rrrc	RRRC	RRID:RRRC_00699
Rat: Wildtype: F344	Janvier Labs	RRID:RGD_60994
Software and algorithms		
SMART Video Tracking v3.0.06	Panlab	RRID:SCR_002852
Stereo Investigator	Leica	RRID:SCR_002526
LAS X software	Leica	RRID:SCR_013673
GraphPad Prism version v10.4.1	Prism	RRID:SCR_002798
ANTs	NA	RRID:SCR_004757
MRTrix3	NA	RRID:SCR_024123
Nilearn	NA	RRID:SCR_001362
ITK-SNAP software v3.8.0	NA	RRID:SCR_002010
ImageJ v2.14.0/1.54f; Java 1.8.0_322 (64-bit)	NA	RRID:SCR_003070

EXPERIMENTAL MODEL AND STUDY PARTICIPANT DETAILS

Animals and experimental design

Male and female TgF344-AD rats (n = 30) and wild-type (WT) Fischer littermate rats (n = 30) were group-housed under controlled conditions of temperature (22 ± 1°C) and humidity (55 ± 10%) on a 12 h light/12 h dark cycle from the time they were 3 months old. Water and food were available *ad libitum* except during behavioral tests. Animal work was performed in accordance with the local legislation (Decret 214/1997 of July 30th by the Departament d'Agricultura, Ramaderia i Pesca de la Generalitat de Catalunya)

with the approval of the Experimental Animal Ethical Committee of the University of Barcelona, and in compliance with European legislation.

MRI scans were performed at 5 timepoints: 3, 7, 11, 15 and 19-months-old, with the first scan being performed before DNMS training. Littermates were randomly divided into two groups: untrained and cognitively trained by repeated performance of the DNMS task in operant chambers. At 3 months of age rats underwent the habituation and the DNMS training. All animals passed the acquisition criteria and reached the DNMS phase, which was performed for 10 consecutive days at 7,11, 15 and 19 months of age. At 7 months old, rats performed the DNMS task for 10 consecutive days every 4 months. The novel object recognition (NOR) test was performed at 19 months for all experimental groups, after which rats were sacrificed and their brains extracted for histological and protein assays. A small subgroup of rats (n = 3–4 per experimental group) was sacrificed at 11 months to study the effects of cognitive training over beta-amyloid burden and microglia in middle adulthood (Figure 1). A specific breakdown of the number of animals used in each experiment can be found in Table S1.

METHOD DETAILS

Training and delayed non-match to sample task

Cognitive stimulation was performed by training to acquire DNMS task and periodical repetition of DNMS performance, starting at 3 months of age until 19 months of age. The task was performed in isolated operant chambers (Med Associates, Fairfax, VT, USA) containing 3 extendable levers: two were placed on the pellet wall (right and left levers) and the third was centered on the opposite wall. Rats underwent habituation, training and task phases as previously described.[20] In brief, the habituation phase involved exposing the rats to 5 min of daily handling for 7 days and placing them in the DNMS chambers for 30 min. During the testing weeks, the animals received 75% of their standard food intake to increase their performance motivation. The DNMS training phase consisted of six levels of ascending difficulty. The DNMS task was initiated when acquisition criteria were satisfied.[20] Namely, 2 consecutive days with a score of a minimum of 80% correct responses in the 5th and 6th training phases, where the procedure is identical to DNMS but with no delay or delay between 1 and 5 s, respectively. All animals achieved the criteria and reached the DNMS phase. The DNMS task started with the sample phase, where the animals had to press the lever that extended (left or right). After a random 1 to 30-s wait, the center-placed lever on the opposite wall would extend, and the rats had to press it. If successful, both right and left levers would extend again, and the rats had to press the lever which had not been presented during the sample phase (non-matched) to obtain a sucrose pellet reward. An incorrect response (pressing the matched lever) led to a 5-s time-out with overhead lights turned off and no pellet reward. The DNMS tasks were finalized after 60 min, or 90 trials were performed.

Novel object recognition test

The NOR test was used to evaluate the rat's recognition memory. At 19-months-old, rats were individually placed in empty testing arenas (40 cm × 40 cm x 30 cm) for 5 min for habituation purposes. Familiarization and testing phase were performed the following day, where the rats were placed in the testing arena for 5 min with two identical objects. After a 30-min delay, rats were placed back in the arena with the following two objects: a familiar one (from the familiarization phase) and a novel object. The interaction with these objects was recorded for 5 min with a digital video camera mounted overhead. The SMART 3.0.06 video tracking software (Panlab) was used to analyze the recordings and track the time each rat spent exploring each object, to quantify the recognition index (RI), the time spent interacting with the novel object relative to the time spent interacting with both, as well as the total exploration time. Object exploration was counted when rats were within a 2 cm perimeter of an object, with their snout directed toward it. For analysis purposes, only the first 2.5 min of each 5-min recording were used, as the rats lost interest and showed reduced locomotor activity over time, potentially masking cognitive deficits between the experimental groups.[43]

Magnetic resonance imaging

MRI experiments for functional connectomics were performed as previously described on a 7.0-T BioSpec 70/30 horizontal animal scanner (Bruker BioSpin, Ettlingen, Germany) equipped with an actively shielded gradient system (400 mT/m, 12-cm inner diameter).[20] Briefly, animals were placed in a prone position in a Plexiglas holder with a nose cone for administering anesthetic gases (1.5% isoflurane in a mixture of 30% O_2 and 70% CO_2) and were fixed using tooth, ear bars and adhesive tape. To ensure stability during the resting state functional magnetic resonance imaging (rsfMRI), rats received a 0.5 mL bolus of medetomidine (0.05 mg/kg; subcutaneously (s.c.)) and a catheter was implanted in their back for continuous perfusion of medetomidine. Isoflurane was gradually decreased to 0.5% and 15 min after the bolus, the medetomidine perfusion (0.1 mg/kg/h; s.c.) started at a rate of 1 mL/h. The acquisition protocol included the following imaging: T2-weighted images, acquired using a rapid acquisition with relaxation enhancement (RARE) sequence with effective echo time (TE) of 35.3 ms, repetition time (TR) of 6000 ms, RARE factor = 8, voxel size = 0.12 × 0.12 mm^2, 40 slices, slice thickness = 0.8 mm and field of view (FoV) = 30 × 30 × 32 mm^3; T1-weighted images, acquired using an Modified Driven Equilibrium Fourier Transform (MDEFT) protocol with TE = 2 ms, TR = 4000 ms, voxel size = 0.14 × 0.14 × 0.5 mm^3 and FoV = 35 × 35 × 18 mm^3. For rsfMRI, a gradient echo T2* acquisition was used, with the following parameters: TE = 28 ms, TR = 2000 ms, 600 volumes (20 min), voxel size = 0.4 × 0.4 × 0.6 mm^3, FoV = 25.6 × 25.6 × 20.4 mm^3.

Image processing and connectome definition

The acquired images were processed to obtain the functional connectomes. Briefly, at each age timepoint, a T2-weighted group template was constructed by interactive multi-stage registration using ANTs,[85] and a modified SIGMA rat brain atlas was registered to the corresponding group template.[86] Then the atlas parcellation and segmentation were registered to each subject's T2-weighted images using the group template as an intermediate registration step to obtain individual brain masks and region parcellations. RsfMRI volumes were denoised, skull-stripped and intensity-normalized using MRTrix3.[87] Atlas parcellation and segmentation were registered from each subject's T2 space to their respective pre-processed rsfMRI spaces to define the regions between which connectivity was assessed.

RsfMRI processing was done with Nilearn.[88] Time series were detrended and standardized, a band-pass filter was applied to keep frequencies between 0.01 and 0.1Hz and a Gaussian smoothing kernel was applied with a full width at half maximum of 1 mm to enhance signal-to-noise ratio and increase statistical sensitivity.

Brain activity identified by rsfMRI has been constrained to gray matter tissue,[89] thus 94 regions were considered as nodes in the functional connectome. The connection weight between nodes was calculated as the partial correlation between the pair of regional time series, converted to z-scores by applying Fisher's z-transformation. Because the correlations are symmetric, undirected graphs were constructed. Negative correlation coefficients were excluded since negative functional connectivity has potentially artifactual origins and unclear physiological interpretation. All the connections with positive weight ($z > 0$) were considered for weighted undirected functional connectome construction. Binary undirected functional connectomes were constructed by setting all non-zero values of their weighted counterparts to 1.

Connectome metrics

Brain network organization was described using graph theory, taking different brain regions as nodes and functional connectivity as vertices. This allows us to study functional connectivity at the network level by capturing the complex and dynamic interplay between brain regions in a systematic and quantifiable manner. Specially, we focused on global efficiency and clustering coefficient. These metrics provide a description of integration and segregation at a global level.[90] Global efficiency measures network integration or the ability to combine information from different regions. It is inversely related to the shortest path length and it is calculated as the average efficiency between all pairs of nodes. A higher global efficiency characterizes stronger and faster communication through the network. Network segregation, which is the ability of specialized processing within densely interconnected groups of regions, was quantified by the clustering coefficient. The average clustering coefficient is the average of nodal clustering coefficients, which are calculated as the fraction of possible triangles that exist between each node and its neighbors (triangles being sets of three nodes that are all mutually connected by edges). High clustering coefficient values are related to highly segregated and connected networks. These metrics have been commonly used in human studies of AD,[91–94] and therefore, can provide comparable and translational results. For longitudinal functional network metrics comparison between groups, 5 data points from different subjects were discarded due to MRI acquisition and processing issues.

Seed-based analysis of the EC and the DG

Seed-based analysis is a model-based method in which a region of interest (ROI) is selected as a seed and correlations between its average blood-oxygen-level-dependent (BOLD) signal and the BOLD signal of all brain voxels are calculated.[95] Seed-based analyses were performed using the left entorhinal cortex (EC) and the left dentate gyrus of the hippocampus as two independent seeds, segmented from the rat brain MRI atlas[86] to build a seed-based functional connectivity map, providing information on which brain regions are functionally connected. Correlation maps were calculated using the Nilearn package and were converted to z-scores using Fischer's transformation. A non-parametric permutation inference procedure[96] was applied to determine which brain regions showed different connectivity patterns between groups by implementing a non-parametric *t* test with a total of 5000 permutations per contrast. The resulting *p*-values maps were then processed to detect cluster-like structures using the Threshold-Free Cluster Enhancer (TFCE) procedure,[97] and multiple comparisons were adjusted by controlling the Family-Wise Error (FWE) Rate ($\alpha = 0.05$). Images were visualized using the ITK-SNAP software (version 3.8.0).[98]

Tissue preparation

At 11 ($n = 16$) and 19 ($n = 43$) months, after the corresponding MRI session with rats under deep anesthesia, transcardiac perfusions were performed with phosphate-buffered saline (PBS) washes and with 4% paraformaldehyde. Rats were decapitated and brains were extracted. Both hemispheres were separated, one for histological studies and the other was dissected, quickly frozen, and stored at −80°C for biochemical studies. The hemisphere used for histological studies was coronally cut into 6 slices of 3 mm, excluding the cerebellum. The slices were mounted on paraffin blocks (Leica EG 1150H) and subsequently sliced into 5 μm sections using a microtome (Leica RM2255).

Immunohistochemical studies

Deparaffinized 5 μm coronal sections were incubated with PTlink at pH 6 (20 min at 95°C) and then with 98% formic acid (5 min). A peroxidase blocking solution (Dako) incubation was performed (30 min) before the 45-min incubations with primary antibodies; rabbit anti-NeuN (1:1000; Abcam, #177487) or mouse anti-Aβ (1:100; Dako, #M0872). For signal amplification rabbit (Dako, #K8009) or

mouse linker (Dako, #K8021) were added (30 min), prior to incubations with horseradish peroxidase (HRP)-linked goat anti-rabbit (Cell Signaling Technology, #7074) or anti-mouse (Thermo Fisher Scientific, #32430) secondary antibodies (30 min). 3,3′-Diaminobenzidine (DAB) chromogen was added (10 min) and slides were stained with hematoxylin. Washes with Dako buffer were performed between incubations. The tissues were mounted onto slides, dehydrated, and covered with coverslips ready for microscopy use. All steps were performed in a humid chamber at room temperature (unless stated otherwise) in the dark until DAB was added.

Immunofluorescence studies

Deparaffinised coronal sections were incubated with PTlink (20 min at 95°C) followed by an incubation with 98% formic acid (5 min). LinkerMouse incubation was followed by a 1 h 5% bovine serum albumin (BSA) incubation and 45-min incubation with primary antibodies; mouse anti-Aβ (1:100; Dako, Clone #M0872), rabbit anti-Iba1 (1:400; Wako, #019–19741) and rabbit anti-parvalbumin (1:500; Proteintech, #29312-1-AP). Sections were incubated for 1 h in the dark with goat anti-mouse Alexa Fluor 488 (1:400; Thermo Fisher Scientific, #A31620), or donkey anti-rabbit Alexa Fluor 546 secondary antibodies (1:400; Thermo Fisher Scientific, #A10040). Sections were rinsed in 70% ethanol for 5 min and stained with saturated (70% EtOH) Sudan Black solution for 15 min. Slides were rinsed and cover-slipped with Fluoroshield with DAPI mounting medium (Sigma-Aldrich, #F6057).

Image acquisition and analysis

For $NeuN^+$ cell count and quantification of microglia to plaque size ratio, the BX-51 Biological Binocular Microscope (Olympus) was used. For unbiassed $NeuN^+$ count, the optical fractionator technique was applied using the Stereo Investigator Software (Leica). The 4× objective was used to obtain $NeuN^+$ images of the areas of the EC and hippocampus (DG, CA1, CA3). One image was acquired per region per animal. For quantification, the perimeter of each area was delimited as a ROI, and using the 20× objective a randomized grid-counting system was used to estimate the total neuronal population per area. For each area, the estimated neuronal population was then normalized to its respective ROI to obtain a $NeuN^+$ count/area. To obtain images of microglia around Aβ plaques, the 40× objective was used to acquire an image per region per animal. For each image, a pre-determined ROI was placed around each Aβ plaque, and the microglia within were considered as plaque associated. Images of parvalbumin-positive (PV^+) cells were acquired using a widefield AF6000 optical microscope (Leica) at 20× magnification. The LAS X software (Leica) was used to obtain a mosaic of the hippocampus (DG, CA1, CA3), for each animal. PV^+ interneuron counts were then performed manually on ImageJ software (version 2.14.0/1.54f; Java 1.8.0_322 (64-bit)). Total PV^+ interneuron counts per region were normalized to their respective ROIs to obtain a ratio of PV^+ counts/area. The confocal SP5 2 photon microscope (Leica) was used to generate 3D images of $Iba1^+$ microglial cells in the EC. The rhinal fissure served as anatomical reference, and images were acquired in a ventral direction. The 40× oil-immersed objective was used to obtain 4 images per rat. Images were 1,024 × 1,024 pixels, obtained at a 400 Hz speed with z-stacks using the LAS X software. Images of the hippocampus (DG, CA1, CA3) were obtained in - 3.2 mm bregma, and of the EC in −5.2 mm bregma, based on bregma coordinates from the Paxinos and Watson's Atlas of Stereotaxic Surgery.[99] ImageJ was used to process and analyze the acquired images. For the analysis of microglial morphology, the macros "macro.ijm" and "composite_macro.ijm" were used. The plugin "AnalyzeSkeleton 2D/3D" was used to binarize and skeletonize images for the quantification of branch numbers. Eight microglia were analyzed per subject and the average per rat was analyzed and expressed graphically.

Western Blot analyses

Brain cortical segments mainly including somatosensory, auditory, insular and EC (bregma 1 to −3.55) and the hippocampus (bregma −2.30 to −6.30) were used for Western Blots. The supernatant for analysis was obtained by defrosting samples with an adapted lysis buffer.[100] Samples were then sonicated, incubated for 2 h at 90°C and 300 rpm and centrifugated at 4°C and 1000 g for 10 min. The total concentration of the supernatant was quantified with the DC protein assay kit (Bio-Rad, #5000112), using BSA for the calibration curve (Bio-Rad, #5000007) and following manufacturer's instructions. Aliquots were stored at −80°C until use.

Samples obtained from the rats' cortex (15–20 μg of protein) were separated in NuPAGE™Novex™ 4–12% SDS-acrylamide gels and proteins were transferred to nitrocellulose membranes with the iBlot dry blotting system (Thermo Fisher Scientific). Primary antibodies were diluted in Tris-buffered saline containing 0.1% Tween 20 and 5% BSA and incubated overnight at 4°C. Secondary antibodies were diluted in TBS-Tween with non-fat, dry 5% milk (Bio-Rad) for 1 h. Supersignal West Pico Plus chemiluminescent substrate (Thermo Scientific, #34577) was used for protein detection and images were obtained using ChemiDoc (Bio-Rad). The following primary antibodies were used at a 1:1000 dilution: mouse anti-PSD95 (Thermo Fisher Scientific, #MA1-045), rabbit anti-VGLUT1 (Synaptic Systems, #135303), rabbit anti-p-RPS6 (Ser235/236) (Cell Signaling Technology, #4858), mouse anti-RPS6 (Cell Signaling Technology, #2317), and mouse anti-TrkB (BD Biosciences, #610102). For secondary antibodies, HRP-linked goat anti-mouse (Thermo Fisher Scientific, #31430) and anti-rabbit (Thermo Fisher Scientific, #31460) were used at a 1:10000 dilution.

ImageJ was used for image analysis and the quantification of relative protein expression obtained from Western blots.

QUANTIFICATION AND STATISTICAL ANALYSIS

Analyses were performed using a mixed-effect model, a two-way ANOVA, or three-way ANOVA, depending on the number of factors analyzed, as specified in each figure legend. When appropriate, post hoc Tukey tests were conducted following two-way ANOVA, and Fisher's least significant difference (Fisher's LSD) tests were performed following three-way ANOVA. Data was analyzed

separately by sex except in histological studies where the 11 months-old groups were too small to divide by sex. To investigate the relationship between RI at 19 months and global efficiency metrics at 7 and 11 months, Pearson's correlations coefficients were calculated. Data was processed and analyzed blindly. Statistical analyses were performed with the GraphPad Prism 10 software (version 10.4.1) and data were presented as mean ± standard error of the mean (SEM), considering $p < 0.05$ as statistically significant. Unless specifically stated, '*' were used to indicate statistical significance between treatments and '#' were used to indicate statistical significance between sexes, where *$p < 0.05$; **$p < 0.01$; ***$p < 0.005$ and #$p < 0.05$; ##$p < 0.01$; ###$p < 0.001$.The complete results from the ANOVAs, including F-values, degrees of freedom and p-values, are available in the supplementary tables.